City Research Online

City, University of London Institutional Repository

Luminance contrast drives interactions between perception and working memory

Maciej Kosilo[1,2], Jasna Martinovic[3], Corinna Haenschel[1]

1 School of Arts and Social Sciences, Department of Psychology, City, University of London, Northampton Square, London EC1V 0HB, UK

2 Institute of Biophysics and Biomedical Engineering, Faculty of Sciences, University of Lisbon, Campo Grande, Lisbon, 1794-016, Portugal

3 Department of Psychology, School of Philosophy, Psychology and Language Sciences, University of Edinburgh, 7 George Square, Edinburgh, EH8 9JZ, UK

Address the correspondence to: m.kosilo@gmail.com, tel. +351 966 914 553

Institute of Biophysics and Biomedical Engineering

Faculty of Sciences – University of Lisbon

Campo Grande

1749-016 Lisbon, Portugal

ABSTRACT

Visual working memory enables the use of past sensory experience in guiding behaviour. Yet laboratory tasks commonly evaluate working memory (WM) in a way that separates it from its sensory bottleneck. To understand how perception interacts with visual memory, we used a delayed shape recognition task to probe how WM may differ for stimuli that bias processing towards different visual pathways. Luminance compared to chromatic signals are more efficient in driving the processing of shapes and may thus also lead to better WM encoding, maintenance, and memory recognition. To evaluate this prediction, we conducted two experiments. In the first psychophysical experiment, we measured contrast thresholds for different WM loads. Luminance contrast was encoded into WM more efficiently than chromatic contrast, even when both sets of stimuli were equated for discriminability. In the second experiment, which also equated stimuli for discriminability, early sensory responses in the electroencephalogram (EEG) that are specific to luminance pathways were modulated by WM load and thus likely reflect the neural substrate of the increased efficiency. Our results cannot be accounted for by simple saliency differences between luminance and colour. Rather, they provide evidence for a direct connection between low-level perceptual mechanisms and WM by showing a crucial role of luminance for forming WM representations of shape.

Keywords: EEG, Psychophysics, Visual Perception, Visual Working Memory, luminance, colour, shape perception

INTRODUCTION

Visual working memory (visual WM) is the ability to encode, retain and manipulate information for a brief period and is fundamental for performing many everyday tasks (Baddeley, 2003, 2010; Baddeley & Hitch, 1974; Logie, 2011; Phillips, 1974). The sensory recruitment hypothesis suggests that the same mechanisms that are important for forming

2

the initial sensory representation are also active during the maintenance of the information (D'Esposito & Postle, 2015; Harrison, Tong, 2009; Katus, Grubert, & Eimer, 2015; Pasternak & Greenlee, 2005). While the hypothesis itself is debated (e.g. Harrison & Bays, 2017, Yörük et al., 2020), it challenged the idea that perception and WM are separate constructs, further supporting the notion that they are dynamically interacting processes (Albers, Kok, Toni, Dijkerman, & de Lange, 2013; Gao, Gao, Li, Sun, & Shen, 2011; Lara & Wallis, 2015; Scimeca, Kiyonaga & D'Esposito, 2018; Yin et al., 2012). This recently shifted the research focus towards clarifying the relationship between perception and WM (e.g. Rademaker, Chunharas & Serences, 2019, Constant & Liesefeld 2021).

Nevertheless, most research up to date focuses on investigating the retention stage of WM and the location of memory storage, while perceptual factors contributing to a successful encoding of the stimulus are less understood (Christophel, Klink, Spitzer, Roelfsema, & Haynes, 2017; Luria, Balaban, Awh, & Vogel, 2016). However, a recent study by Constant & Liesefeld (2021) showed that bottom-up visual saliency of the to-be-remembered stimulus impacts WM performance, suggesting that low-level mechanisms may make an important contribution to WM representations. This study clearly demonstrated the importance of studying low-level factors in WM during perceptual encoding and is in line with research suggesting that perception and visual WM should be viewed as dynamically interacting, rather than as separate processes. We aim to extend this understanding by evaluating interactions between perception and WM at the earliest stages of visual processing.

At the most basic level of visual perception, a coherent representation of the environment is constructed from the information arriving in the cortex via multiple parallel channels from the retina through the lateral geniculate nucleus. In low-level vision, three main retinogeniculate pathways in the human visual system (magno, parvo and koniocellular) have been related to the three psychophysically identified post-receptoral mechanisms (for an overview, see Martinovic, 2016). These are the luminance mechanism and two cone-opponent mechanisms ("reddish-greenish" and "bluish-yellowish"; De Valois & Kooi, 1991; Derrington,

Krauskopf, & Lennie, 1984; Livingstone & Hubel, 1987).[1] These mechanisms process signals that originate from the three cone types in the retina (long, medium, short-wavelength cones, or L, M and S, respectively): the luminance mechanism combines signals from L and M cones (L+M), while the chromatic mechanisms compare information from cones sensitive to different parts of the visible spectrum (L-M for "reddish-greenish" and S-(L+M) for "bluish-yellowish").

Within vision research, the aim is to determine whether these mechanisms are equally efficient in sustaining different perceptual processes (Crognale, 2002; Gegenfurtner & Kiper, 2003; McKeefry, Murray, & Kulikowski, 2001; Vidyasagar, Kulikowski, Lipnicki, & Dreher, 2002). Here, we introduce this approach to the WM domain. Luminance signals contribute to global shape discrimination (Mullen & Beaudot, 2002) and detection of edges and motion (Gegenfurtner & Rieger, 2000) more efficiently than chromatic signals. Furthermore, they benefit high-level processes, such as object recognition. This is usually demonstrated through faster and more accurate classification and discrimination of objects from non-objects (Kveraga, Boshyan, & Bar, 2007; Martinovic et al., 2011; Jennings & Martinovic, 2014). Because conduction is faster for the magno cells compared to the parvo cells, a magnocellular 'speed advantage' has been proposed (Bar, 2003; Laycock, Crewther, & Crewther, 2008, 2007; Maunsell et al., 1999). This allows fast feedforward connections but also cortical interactions via feedback (modulating the slower arrival of information by parvocellular activity) at different levels of the visual system (for a review, see Grinter, Maybery, & Badcock, 2010). The feedforward connections have been suggested to provide a fast and automatic initial global analysis of the visual scene, which then enables attentional mechanisms to modulate the responses. In line with this, it was suggested that the benefit of

---

[1] Note that the three psychophysical channels do not perfectly map onto the anatomical magno, parvo and koniocellular pathways; for example, although it is true that magnocellular pathway takes mostly the luminance information, it does not mean that the parvocellular pathway is not capable of processing luminance contrast, in addition to chromatic contrast (see e.g. Lee & Sun, 2009; Schiller & Corby, 1983).

luminance in object recognition is mediated through the fast projections into the prefrontal cortex (Kveraga et al., 2007).

Since WM relies on a widely distributed network of brain areas (Eriksson, Vogel, Lansner, Bergström, & Nyberg, 2015), including the prefrontal cortex as well as the early sensory areas (Harrison & Tong, 2009; Pasternak & Greenlee, 2005), luminance signals likely have particular relevance for WM processing, parallel to their special role in perception. However, the influence of these low-level visual mechanisms on WM performance has not been directly investigated. Previous work used event-related potentials (ERP) to probe the early perceptual stages and the later, memory-related operations using a delayed recognition task (Haenschel et al., 2007). In Haenschel et al. (2007), which used luminance-defined stimuli, the early visual P1 component was predictive of successful WM encoding.

P1 indexes early visual processing and is responsive to low-level stimulus properties like contrast (Ellemberg & Hammarrenger, 2001; Luck, 2014; Shawkat & Kriss, 2000; Souza, Gomes, Saito, da Silva Filho, & Silveira, 2007) and luminance (Johannes, Münte, Heinze, & Mangun, 1995). In fact, the P1 is greatly attenuated or absent in response to isoluminant stimuli, thus making it a perfect candidate ERP signature to track luminance processing (Berninger et al., 1989; Martinovic et al., 2011; Murray, Parry, Carden, & Kulikowski, 1986; Tobimatsu, Tomoda, & Kato, 1995, 1996). In addition to feedforward effects, the P1 has also been related to the suppression of irrelevant information in spatial attention (Fukuda & Vogel, 2009; Hillyard, Vogel, & Luck, 1998; Johannes et al., 1995; Mangun, Hillyard & Luck, 1993) and perceptual load (Handy & Mangun, 2000). Other studies have also demonstrated prefrontal facilitation of the P1 (Barcelo, Suwazono, & Knight, 2000; Zanto, Rubens, Thangavel, & Gazzaley, 2011). Moreover, an fMRI study found functional connectivity between the prefrontal cortex and visual cortex during encoding (Bittner et al., 2015). Put together, the P1 exhibits strong modulations by both bottom-up and top-down factors.

Whereas the P1 has been related to luminance, the first clear ERP component that can be observed in response to isoluminant stimuli is the subsequent negative shift in polarity,

labelled as the N1 (Berninger et al., 1989; Martinovic et al., 2011; Murray, Parry, Carden, & Kulikowski, 1986). In the absence of any studies examining if similar WM modulations can be obtained at the N1 level for chromatic stimuli, one could speculate that the changes in P1 amplitude associated with WM load may be attributable to luminance contrast exclusively. However, if these links were not exclusive to luminance, or only observable at the early temporal latency of the P1 (~100 ms peak latency, compared to ~170 ms for the N1), modulation of the N1 component with WM load should also be observed, at least for chromatic signals. This would then imply that early stages of WM encoding are not preferentially influenced by luminance signals.

Other components usually investigated in WM research are non-perceptual. They include the P3 component as well as a long-lasting slow wave spanning the memory maintenance period, often labelled as the contra-lateral delay activity (CDA). P3 has been associated with various stages of working memory processing (Bledowski et al., 2006; Kok, 2001). The slow wave has been related to WM capacity and is usually measured as a difference wave (see Luria et al., 2016 for a review), although it can also be observed in tasks that present stimuli foveally (Pinal et al., 2015; Ruchkin, Johnson, Canoune, & Ritter, 1990; Ruchkin, Johnson, Grafman, Canoune, & Ritter, 1992).

Here, we conduct two experiments that employed the delayed recognition task to probe perception/WM interactions using psychophysical and EEG methods. We made a range of predictions. If WM is more efficient for shapes defined by luminance signals as opposed to chromatic signals, this should be reflected in lower thresholds (i.e., level of stimulus contrast required for 75% performance, expressed in multiples of detection threshold) across three levels of WM load. Expressing contrast in detection threshold units is a classical approach when comparing the efficiency of different low-level signals – luminance, reddish-greenish, or bluish-yellowish – in sustaining various spatial vision tasks (Shevell & Kingdom, 2008). Participants are asked to perform the same psychophysical task (e.g. discriminate circularity of a shape; Mullen & Beaudot, 2002) on stimuli defined by luminance, reddish-greenish or

bluish-yellowish modulations. The resulting contrasts are then expressed in units of detection threshold for each mechanism, to control for more basic differences in threshold sensitivity, which also has relevance for suprathreshold salience (Kulikowski, 1976; for more recent work, see Hardman, Toellner & Martinovic, 2020 and Hardman & Martinovic, 2021). We adopted this approach in the first experiment, a psychophysical delayed recognition threshold task.

The same luminance-driven increase in efficiency should also be reflected in early sensory responses in the EEG that are specific to luminance pathways. In the 2nd experiment, we measured ERPs. While our main focus was on indices of WM encoding, we also evaluated neural markers of maintenance and memory recognition. In terms of behaviour, we again predicted benefits in response to luminance-defined stimuli, reflected in better accuracy and faster reaction times, especially at higher WM loads. The differential contributions of the post-receptoral mechanisms to stimulus processing are more prominent when stimuli are presented at low contrast (Ellemberg & Hammarrenger, 2001; Ivanov & Mullen, 2012; Livingstone & Hubel, 1988). To take advantage of that, in Exp. 2 we present the stimuli at two fixed levels of contrast: low and high and investigate how luminance and chromatic stimuli modulate early and late ERPs at different WM loads (one, two or three items) during encoding, maintenance, and memory recognition.

We expect the P1 component amplitude to increase in response to increasing WM load (as shown previously; Haenschel et al., 2007) in response to luminance-defined stimuli. We also expect that the amplitude of the N1 (1st component robustly elicited by isoluminant stimuli) will not show a relationship with WM load for colour defined stimuli. This would confirm that at the early encoding stages, WM predominantly interacts with luminance signals.

Additionally, by looking at later ERP components during encoding (P3b), maintenance (occipital slow wave during retention period) and recognition (P1, N1, and P3b during the processing of the memory probe) we explore whether luminance also differentially contributes to later cognitive processes and WM stages more efficiently than colour

7

GENERAL METHODS

In this section, we outline general methods applicable to both experiments, whereas experiment-specific details are provided in the corresponding sections.

APPARATUS

Experiments were implemented in Matlab (Mathworks, Natick, Massachusetts) running on a Dell Precision PC integrated with a Visage (visual stimulus generator) system. Stimuli were presented on a calibrated cathode ray tube (CRT) monitor (NEC MultiSync FP2141SB) which was linearised with a ColorCal Colorimeter (Cambridge Research Systems, Ltd., Kent, UK). The calibration was verified using a spectroradiometer (SpectroCal, Cambridge Research Systems, Ltd., Kent, UK). The CRT was the only source of light during the experiment. The monitor was kept on for at least 30 minutes beforehand. Participants responded using a button box (Cedrus RB – 740, Cedrus Corporation, San Pedro, USA) while seated 57 cm from the screen in an electrically-shielded chamber.

STIMULI

102 non-natural visual objects were used as stimuli (for previous work see Linden et al., 2003; Haenschel et al., 2007). Shapes were generated by randomly distorting Tetris blocks (Pajitnov, 1985) and were presented at varying orientations to increase the number of stimuli that appeared unique (see *Figure 1 A*).

Stimuli were presented in the centre of the screen (size: 1.34°) against a uniform grey background. The CIE coordinates of the background were set to a value corresponding to standard illuminant D65, and were measured to be x = 0.3113, y = 0.3281, and Lum = 56.39/m2. Derrington-Krauskopf-Lennie colour space (DKL; Derrington, Krauskopf, & Lennie, 1984; see *Figure 1 B*) was used to define low-level stimulus properties. In this space, modulations along the two cone-opponent, chromatic axes produce different colour appearances, the L-M axis producing reddish vs. greenish and the S-(L+M) axis producing bluish vs. yellowish. Luminance is defined along an orthogonal, achromatic axis (L+M). The

L-M mechanism weights the difference between L and M-cone excitations (i.e. L – M). The S – (L+M) mechanism takes the weighted difference between S-cone and summed L and M-cone excitations. The achromatic mechanism sums L and M-cone signals (L + M). We created three classes of stimuli that correspond to these mechanisms ("reddish" for L-M, "bluish" for S-[L+M] and grey for L+M).

DELAYED RECOGNITION TASK

Experiment 1 and Experiment 2 used a delayed recognition task (modified from Haenschel et al., 2007; Linden et al., 2003) and tested three levels of WM load (load 1-3; *Figure* 1 A).
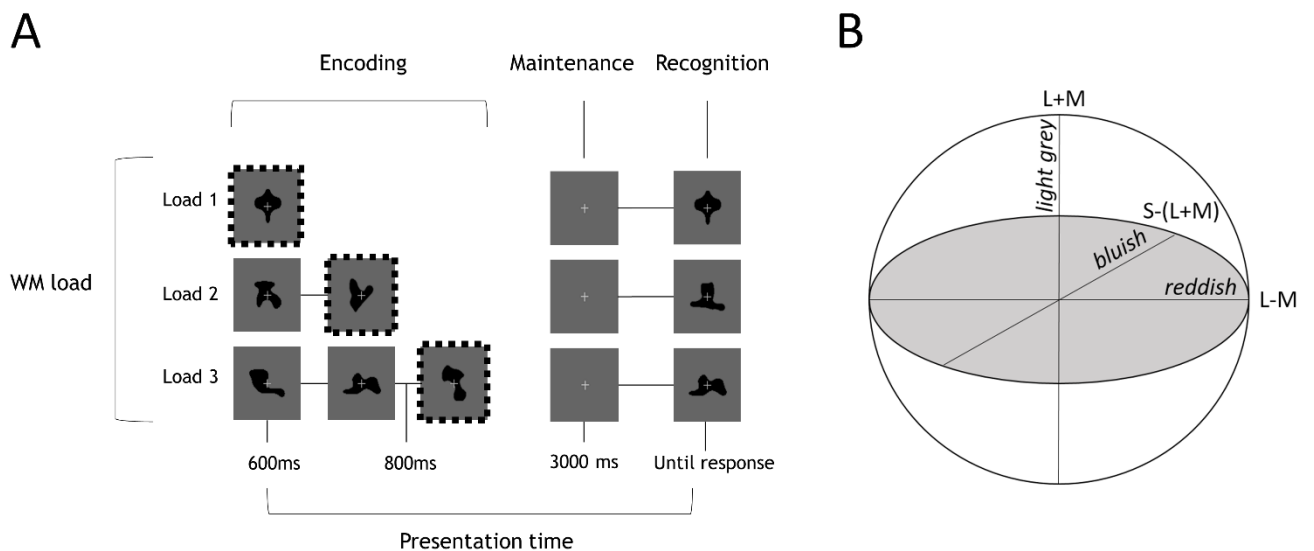

Figure 1. *A)* *Delayed recognition task used in both experiments. On each trial, WM load was manipulated by presenting one, two, or three stimuli in succession for 600 ms each with an inter-stimulus interval of 800 ms (encoding stage). The last stimulus was followed by a 3 s delay (maintenance stage), after which a probe stimulus was presented until a response was made (recognition stage). Participants had to judge whether it was part of the initial sample set ("match") or not ("mismatch") by pressing a button. Dashed-line boxes indicate the ultimate shape in the encoding stage; the encoding and maintenance ERPs were time-locked to the onset of this stimulus. Recognition ERPs were time-locked to the onset of the probe. The dashed boxes are for illustration purposes only and did not appear on the screen during the task. **B)** A schematic representation of the DKL colour space, with the two cone-opponent chromatic axes (L-M; S-(L+M)) and the cone-additive luminance axis (L+M). The isoluminant plane is outlined in grey and the experimental stimuli are labelled in italics.*

SAMPLE SIZE JUSTIFICATION

Sixteen and twenty-two participants were included in the final analysis for Experiment I and II, respectively. Behavioural pilots were conducted to ensure that our study was capable of

reliably capturing differences in performance. Psychophysical pilots were conducted by the experimenters, while the behavioural task for the EEG experiment was piloted on a sample of 12 participants. Furthermore, for a within-subject design such as the one here, past research investigating working memory using EEG used similar sample sizes or lower (Berggren & Eimer, 2016; Feldmann-Wustefeld, Vogel, & Awh, 2018). For example, at 80% power, with a sample of 20 participants, Feldmann-Wustefeld, Vogel, and Awh (2018) could observe a simple within-subject difference of d = 0.66. Berggren and Eimer (2016) with a sample of twelve and fourteen participants in both their experiments could observe a simple within-subject difference of d = 0.89 and d = 0.81, respectively. With our sixteen and twenty-two participants, at 80% power, we could obtain a simple within-subject difference of d = 0.81 and d = 0.63, respectively. Perceptual experiments are usually interested in large effect sizes (e.g. Baker, Lygo, Meese & Georgeson, 2018). Furthermore, power in within-trial designs can be positively affected by the relatively large number of trials used to obtain measurements (Baker et al., 2018). Therefore, we deemed our design sufficiently powered to reveal any effects of note (Lakens, 2021).

P-VALUE CORRECTION AND CONFIDENCE INTERVALS

P-values were corrected using Bonferroni-Holm correction for multiple comparisons (Holm, 1979), implemented in *stats* package for *R* (function *p.adjust*; R Core Team, 2021). The uncorrected p-values are ordered from smallest to greatest and then multiplied by (n – rank +1).

All error bars in box and line plots (in both Exp. 1 and Exp 2) are 95% within-subject confidence intervals (Cousineau 2005; Morey, 2008). All box plots are generated using a *notBoxPlot* Matlab function (Campbell, 2017), modified by us to incorporate the within-subject confidence intervals.

EXPERIMENT 1: WORKING MEMORY THRESHOLDS

METHODS
PARTICIPANTS

Twenty participants were recruited for the study. Sixteen participants (13 women, aged 17 – 31 years, median age 21 years; all right-handed) were included in the final analysis. Four participants were excluded as their thresholds could not be reliably estimated. All participants reported having normal or corrected-to-normal visual acuity and colour vision. This was confirmed using Acuity Plus and City University Colour test (CAD; Barbur, Rodriguez-Carmona & Harlow, 2006). Informed written consent was obtained from each participant. Ethics approval was obtained from the Department of Psychology Research Ethics Committee, City, University of London.

PROCEDURE

The first session consisted of vision tests (AcuityPlus and CAD, mentioned above) to determine whether participants have sufficient contrast sensitivity and typical colour vision, heterochromatic flicker photometry procedure (HCFP; Walsh, 1958) to obtain values needed to minimise luminance artifacts in the luminance stimuli, and the WM threshold measurements. In the second session, we measured detection thresholds that were then used as a baseline for the working memory thresholds for chromatic and achromatic contrasts.

HETEROCHROMATIC FICKER PHOTOMETRY (HCFP)

Individuals differ in terms of their luminous efficiency function (Wyszecki & Stiles, 1982). As a result, luminance artifacts can be present in nominally isoluminant chromatic signals. Heterochromatic flicker photometry (HCFP; Walsh, 1958) was used to adjust the individual's point of isoluminance (e.g. Kosilo et al., 2013; Martinovic et al., 2011; Ruppertsberg, Wuerger, & Bertamini, 2003; Wuerger, Ruppertsberg, Malek, Bertamini & Martinovic, 2011). HCFP takes advantage of the superior temporal resolution of the luminance channel over

cone-opponent channels. Unlike the chromatic systems, the luminance system can detect fast temporal changes, such as flickering at high frequencies. Participants adjusted luminance contrast of a chromatic stimulus flickering at 20 Hz against the background so that the perception of the flicker was minimised. Participants did in total 8 to 10 adjustments per colour, the highest and lowest value were removed as outliers and the average of the remaining measurements was taken and used to adjust the stimulus to isoluminance.

DETECTION THRESHOLDS

We used a 2IFC detection threshold procedure (see *Figure 2*) to measure contrast detection thresholds for each mechanism. The purpose of this procedure was to provide a baseline threshold that we later used to normalise WM thresholds measured in the next experiment. A fixation cross was displayed for 1000 ms. Then participants saw two intervals in succession, each one lasting 600 ms and with an 800 ms fixation period in between. The intervals were indicated by the disappearance of the fixation cross. One of the two 600 ms intervals contained a shape. Participants were required to respond whether the shape appeared in the first or the second interval using the button box bimanually. Auditory feedback was provided for both correct and incorrect answers. The control of the stimulus intensity was based on participants' responses and was adjusted using an adaptive staircase procedure from the Palamedes toolbox (Prins & Kingdom, 2018), with one staircase for each post-receptoral mechanism (luminance and two chromatic). Staircases were interleaved, with the next trial chosen at random from those staircases that had not yet terminated. Each staircase controlled the stimulus contrast for a given condition and was terminated after 35 trials. Participants were told to guess if they were not sure of the answer.

Logistic functions were fitted to data to obtain detection thresholds, i.e. the stimulus contrast at which the probability of correct answer for that individual was 75%.
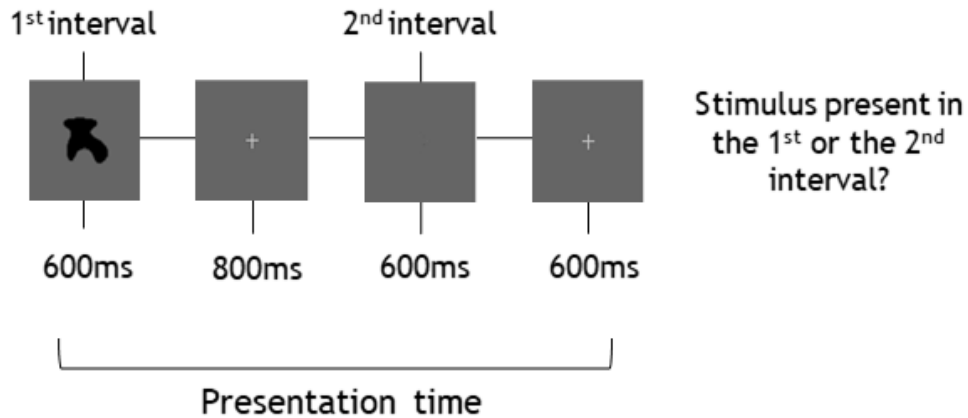
Figure 2. *Two interval forced-choice procedure (2IFC) used to measure stimulus detection thresholds. Two intervals lasting 600 ms were separated by an 800 ms delay with fixation cross. Stimulus was presented either in the 1st or the 2nd interval. Participants were required to indicate which interval contained the stimulus.*

WORKING MEMORY THRESHOLDS

WM thresholds reflected stimulus contrast required for 75% performance in a delayed recognition task (see above) at three levels of WM load. There were nine experimental conditions: three stimulus classes (luminance-defined, "reddish", and "bluish") were presented at WM load 1, 2 and 3. One staircase for each condition, controlled through Palamedes toolbox (Prins & Kingdom, 2018) was interleaved in the procedure, and the stimulus intensity was based on participants' responses and adjusted adaptively, just like in the Detection Threshold procedure. The same intensity was used for every shape presented in a trial. Some WM thresholds could not be estimated during the first session, as some of the staircases failed to converge. In these cases, the range of values to be tested by the adaptive staircase was adjusted and the missing thresholds were re-assessed in a second experimental session.

For the WM thresholds to be meaningfully comparable between luminance and chromatic stimuli, it is important to express them in the same units. This is normally done by measuring a more basic threshold (most commonly, detection threshold) and then expressing the measured contrasts within each mechanism in threshold units (for a review, see Shevell and

Kingdom, 2008). This was done by dividing each staircase value (of each of the 35 trials) by the corresponding mechanism's detection threshold. Subsequently, logistic functions were fitted again to such normalised data to obtain WM thresholds, i.e. the stimulus contrast at which the probability of correctly recognising whether the probe was part of the initial set ("match") or not ("mismatch") was 75% for that individual.

Such WM threshold data were then analysed by a 3x3 repeated measures ANOVA with factors post-receptoral mechanism (bluish, reddish, grey) and WM load (1, 2, 3), using Greenhouse-Geisser correction when necessary.

RESULTS

Overall, WM contrast thresholds differed significantly between the mechanisms ($F_{(1.14, 9.16)} = 32.2$, $p < .001$, $\eta^2 = .80$; see *Figure 3*). Luminance thresholds were lower than bluish ($t(15) = -4.06$, $p = 0.003$, $d = 1.01$) and reddish ($t(14) = -3.91$, $p = 0.004$, $d = 1.01$). There was no significant difference between bluish and reddish ($p = .80$). Thresholds increased with increasing WM load for all mechanisms ($F_{(2, 16)} = 82.1$, $p < .001$, $\eta^2 = .91$). This effect was qualified by an interaction between mechanism and WM load ($F_{(1.77, 14.1)} = 11.3$, $p = .002$, $\eta^2 = .58$). Luminance thresholds were significantly lower at all WM loads than bluish (all pairwise comparisons at $< .001$) and reddish thresholds (all $p = .032$). Thresholds measured for reddish were lower than bluish at load 1 ($t(13) = -2.75$, $p = 0.033$, $d = 0.73$) and load 2 ($t(11) = -3.28$, $p = 0.032$, $d = 0.95$), but not at load 3 ($t(10) = 0.88$, $p = 0.40$, $d = 0.26$).
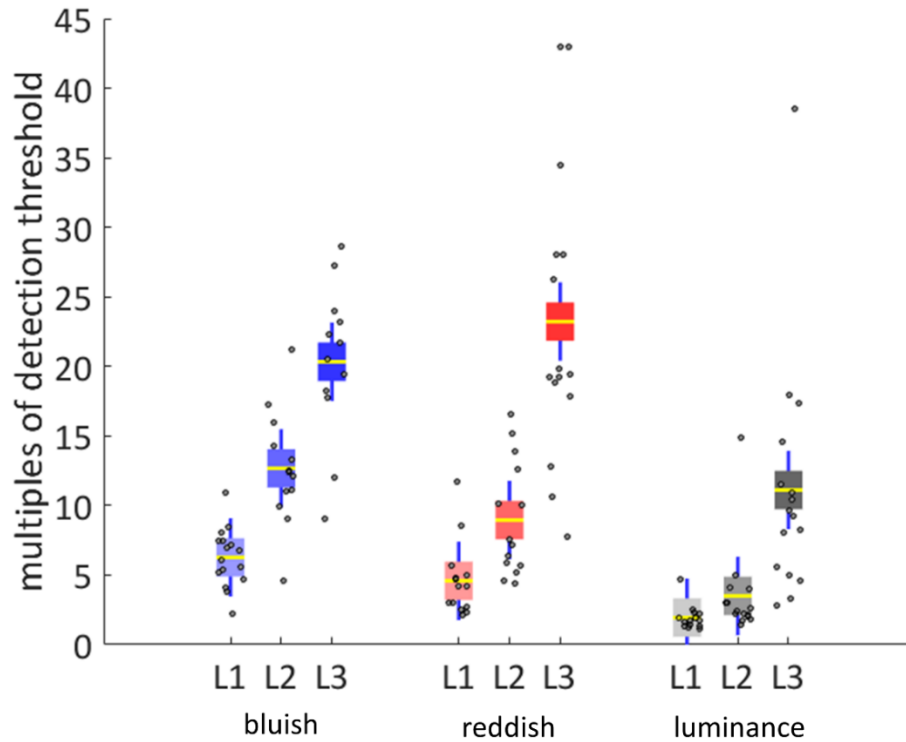
Figure 3. *WM contrast thresholds expressed as multiples of detection thresholds are plotted for the three mechanisms:(bluish (left), reddish (middle) and luminance (right)),at three levels of WM load (L1, L2, L3). Yellow lines are mean WM thresholds across observers, coloured shaded areas are within-subject 95% confidence intervals, and error bars correspond to one standard deviation. Each dot represents an individual observer's WM threshold.*

INTERIM CONCLUSIONS

As can be seen in *Figure 3*, Luminance-defined stimuli required much lower contrast levels to be efficiently encoded into WM. At load 1, it was, on average, 1.95 times the detection threshold for luminance and 4.59 for reddish and 6.27 for bluish stimuli. At load 2, it was 3.5 times the detection threshold for luminance, 8.96 for reddish, and 12.68 for bluish. Notably, at load 3, it was 11.12 times detection threshold for luminance, while for reddish it was 23.23 and for bluish 20.34 times detection threshold. This means that luminance-defined stimuli at load 3 were encoded as efficiently as load 2 stimuli defined by chromatic contrast. This interaction indicates that the source of the effect lies in a more efficient WM process rather than a simple perceptual processing advantage for luminance.

To further examine the interaction between luminance and WM, Experiment 2 matched stimuli for equal salience for every participant and recorded both behavioural data and ERPs

to establish whether this WM-specific advantage for luminance-defined stimuli emerged during encoding, maintenance, and/or memory recognition.

EXPERIMENT 2: AN ERP STUDY OF LOW-LEVEL INPUTS INTO WORKING MEMORY

METHODS
PARTICIPANTS

Twenty-three participants were recruited for the study. One participant had to be excluded as scaled stimulus contrast based on their individual discrimination threshold was outside the monitor's gamut, thus 22 participants (18 women, aged 19 – 51 years [2], median age 25 years; all right-handed) were included in the final analysis. All had a normal or corrected-to-normal vision, which was confirmed using Acuity Plus and City University Colour test (CAD; Barbur, Rodriguez-Carmona & Harlow, 2006). Informed written consent was obtained from each participant. Ethics approval was again obtained from the departmental ethics committee.

PROCEDURE

Participants were tested over three experimental sessions. The first session consisted of vision tests (AcuityPlus and CAD, Barbur, Rodriguez-Carmona & Harlow, 2006) and HCFP (see Experiment 1) as well as the baseline threshold experiment. This session lasted between 2-2.5h. Sessions two and three involved a delayed recognition working memory task with EEG. These two sessions were identical and lasted approximately 3h each (including EEG preparation and breaks). Vision tests and HCFP procedures were described in Methods of Experiment 1.

BASELINE THRESHOLD EXPERIMENT

To equate stimulus salience between luminance and chromatic stimuli, it is best to use a task with similar basic stimulus processing demands. As our WM task required processing of

---

[2] The thresholds measured from the 51-year-old participant were not different from the rest of the participants, thus their data were included in the analysis.

shape, we used same/different shape discrimination thresholds measured for each condition, for every participant. Thresholds were measured using a 2IFC task, four times for each of the three mechanisms. The mechanism to be presented in a given trial (luminance or isoluminant (reddish or bluish) was chosen at random. Participants saw two shapes in succession, each one lasting 650 ms and with a 500 ms fixation period in between and responded whether the shapes were the same or different with a button press.

Stimulus intensities were controlled using an adaptive staircase procedure implemented in the Palamedes toolbox for Matlab (Prins & Kingdom, 2018). Each staircase consisted of 35 trials with auditory feedback for both correct and incorrect responses. To estimate the colour contrast threshold from the relative frequency of a correct response, a Weibull function was fitted to obtain the threshold contrast (defined as the 81% correct point on the psychometric function). The four threshold measures were averaged to obtain a mean threshold for each participant. For some participants and some conditions, the thresholds did not converge; such values were discarded. This was rare. As a result, thresholds for some conditions were based on three rather than four runs (but never less than three).

CONTRAST SCALING PROCEDURE

To achieve a good signal-to-noise ratio in the EEG experiment, contrast thresholds for luminance and chromatic stimuli for the EEG experiment were scaled up while maintaining the relative differences between their intensities. Given that contributions of post-receptoral mechanisms tend to overlap at high contrasts during shape processing (Ivanov & Mullen, 2012), while differences between them may be more prominent at lower contrast levels, we presented stimuli at a high and low contrast level.

Contrasts were scaled from the threshold for each participant to create equivalent low contrast and high contrast stimuli: the luminance stimulus was scaled to a Weber contrast of 0.097 for the low, and 0.194 for the high contrast and then all the other stimuli were scaled using the same scale factor to create a set of equivalent suprathreshold contrasts. These

specific radiuses were chosen based on a pilot study to create low contrast stimuli that would sustain a reasonable level of performance in a working memory task, and high contrast stimuli that were still within the monitor's gamut.

CONTRAST VALUES FOLLOWING THE BASELINE PROCEDURE

Contrasts in each of the mechanisms were calculated from Weber cone contrasts. Contrasts for discrimination thresholds ranged from 0.044 to 0.137 for bluish (0.081 on average), from 0.007 to 0.016 for reddish (0.012 on average) and from 0.030 to 0.062 for luminance (0.044 on average). Scaled contrasts used as the *low contrast* combination ranged from 0.117 to 0.293 for bluish (0.180 on average), while for reddish the contrast went from 0.014 to 0.041 (0.026 on average). The *high contrast* stimuli ranged from 0.234 to 0.586 for bluish (0.360 on average) and for reddish the contrast went from 0.028 to 0.082 (0.052 on average).

Luminance contrasts at threshold ranged from 0.032 to 0.062 (0.044 on average). In the script that ran the experiment, low and high contrast luminance shapes had a fixed DKL radius value, while radii for the chromatic stimuli were scaled based on the threshold to an equivalent level. However, as three participants were tested on slightly different monitor calibration, this meant that their low and high luminance contrast differed slightly from the last set of the participants. Taking these three participants into account, *low* luminance contrasts ranged from 0.097 to 0.102 (0.097 on average), and *high* luminance contrasts ranged from 0.194 to 0.204 (0.195 on average).

WORKING MEMORY DELAYED RECOGNITION TASK

Stimulus contrasts for the WM task were fixed based on threshold measurements. Overall, there were 18 experimental conditions - 3 WM loads (1, 2 or 3 shapes to be remembered), 2 contrast levels (low or high contrast), and 3 mechanisms (luminance, reddish and bluish), each targeting a different low-level mechanism. Furthermore, we also differentiated between match/mismatch (same/different) judgements, i.e., trials where the memory probe either matched the previously remembered stimulus or not.

Trials were presented in a randomised order. Trials with different WM load levels were randomly distributed across two recording sessions with a total of 864 trials (48 trials per condition) obtained per WM load level, visual condition, and contrast level. Half of the 48 trials contained a matching probe, and the other half contained a mismatching probe.

EEG MEAUREMENT, PREPROCESSING, AND ANALYSIS

EEG data were acquired using a 64-electrode ActiCap (Brain Products, Munich, Germany), with the reference electrode at location FCz, the ground electrode at AFz and a vertical ocular electrode placed below the participant's left eye. Electrode impedances were kept below 5kΩ. Recording and digitization were performed using a BrainAmp amplifier and the BrainVision Recorder software (Brain Products, Munich, Germany). The EEG was recorded at 1000 Hz sampling rate with a low-cutoff, hardware filter of 0.016 (1st order filter with a slope of 6 db/octave), and a high-cutoff butterworth filter with 24 db/octave at 450 Hz to prevent aliasing.

Data were further pre-processed using custom-written routines as well as functions derived from EEGLAB (Delorme & Makeig, 2004) and FieldTrip (Oostenveld, Fries, Maris, & Schoffelen, 2011) toolboxes developed for Matlab (Mathworks, Natick, Massachusetts). The two separate EEG recording sessions were merged after pre-processing.

First, non-epoched data was filtered with a high-pass Hamming windowed sinc FIR filter (passband edge: 0.01 Hz; transition bandwidth: 0.01 Hz, cut-off frequency (-6 dB): 0.05 Hz, filter order: 33000), as well as a notch filter to reduce 50 Hz line noise (passband edges: 45 & 55 Hz; transition bandwidth: 2 Hz, cut-off frequencies (-6 dB): 46 & 54 Hz, filter order: 1650).

Noisy electrodes were identified by visual inspection and removed (average of 2 electrodes removed per participant), and data was re-referenced to an average of all electrodes. Major artifacts were removed manually before running the Independent Component Analysis (ICA; Delorme & Makeig, 2004). ICA components reflecting artifacts in the continuous data were selected for removal via visual inspection aided by the SASICA EEGLAB plugin (Chaumon,

Bishop, & Busch, 2015). ICA was performed on continuous data to better capture a range of artifacts that may not only be localised within the epochs: blinks, eye movements and muscle activity. On average, 36 components were removed per participant. This number may appear large, but is in fact not excessive: in the supplementary figure of the SASICA article (Chaumon et al., 2015), it is clear that a large number of artifactual components recommended for rejection explain only a small % of the variance. After ICA subtraction, removed electrodes were reconstructed using spherical spline interpolation, followed by segmenting data into epochs. The EEG data was averaged in epochs from −100 milliseconds before to 600 milliseconds after stimulus onset for encoding and recognition P1 and N1, and between 100 milliseconds to 1700 milliseconds for P3b and retention-related ERP activity. Averaged data were low-pass filtered at 30 Hz. All data were baseline corrected from −100 milliseconds to the stimulus onset. After including only epochs with correct responses, there was on average 33 trials remaining per condition for all ERPs during encoding (range: 27 to 38) and maintenance, 35 trials for recognition P1 and N1 (range: 28 to 41), and 33 for P3b recognition (range: 27 to 38).

To assess encoding, we analysed the final sample stimulus in each WM load condition (see Haenschel et al., 2007). We also analysed the ERP components during the retention (i.e. the time after presentation of the last to-be-remembered stimulus) and the recognition phase (i.e. when the memory probe appears on the screen).

ERPs – MEASUREMENT AND JUSTIFICATION

We based our initial choice of electrode sites and time intervals of each ERP component on Haenschel et al. (2007). To further refine the choice of electrodes and time windows used for our analysis, we averaged the waveforms of all participants and across all experimental conditions, and selected the time range and electrode sites where the amplitude of a given component was the largest (this follows the "collapsed localisers" approach described in Luck & Gaspelin, 2017). We also plotted single-subject waveforms to verify whether ERP peaks fall within the time interval we chose, given that the latency of ERP components varies

between participants (see *Table 1* for a summary of selected electrode clusters and time intervals).

The average voltage of both the P1 and N1 was measured between the peak's onset and offset. These were defined as time points where the voltage reached 50% of the component's peak on either side (a fractional peak latency measure; Kiesel, Miller, Jolicœur, & Brisson, 2008; Luck, 2014). The component peaks were defined as local maxima, i.e. time point which had larger amplitude than two neighbouring samples, detected using Matlab's *findpeaks* function (of the Signal Processing Toolbox; see *Figure 4*). In case more than one local maxima were detected, the largest one was chosen. If no local maxima were detected, the average activity within the time interval was measured instead to avoid missing data. This procedure ensured that both components, which are central to our hypotheses, were measured with good accuracy, considering differences in components' latencies between individuals and between mechanisms. On the other hand, for component P3b and the slow wave, we calculated the mean voltage across the entire time interval, rather than between peaks' onset and offset. This was because these are not as focal as the P1 or the N1, and hence accurately identifying its onset and offset would be problematic.

Table 1 *Electrode clusters and time windows identified for ERP analysis, based on inspection of grand average as well as the topography. Data within the electrode cluster was averaged prior to component measurement. For P1 and N1, the local peaks were identified within a common time interval (see Figure 4), and for P3b and slow wave, a simple average within the common time interval was calculated.*

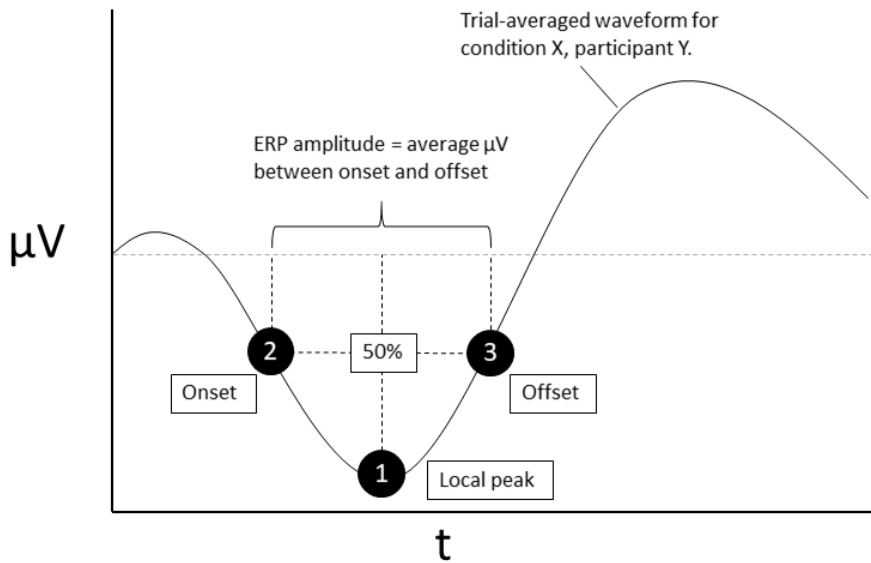|	ERP component	Electrodes	Time interval
Encoding	P1	PO7/8	80 – 160 ms
	N1	O1/2, Oz	130 – 300 ms
	P3b	CP1/2, CPz; P1/2, Pz	200 – 1000 ms
Maintenance	Slow wave	PO7/8; P7/8; P5/6	1000 – 1600 ms
Recognition	P1	PO3/4, POz	80 – 160 ms
	N1	O1/2, Oz	130 – 300 ms
	P3b	CP1/2, CPz; P1/2, Pz	200 – 1000 ms

Figure 4 *Schematic representation of P1 and N1 measurement. For each participant's trial-averaged data, and for every condition, the ERP's onset (1) and offset (2) were then identified in relation to the local peak (3). The local peak was searched for within fixed time interval, which was the same for every participant (see Table 1). Onset and offset are defined as the time point at which the amplitude reached 50% of the local peak. The mean amplitude between those two points was measured and subjected to statistical analysis. Thus, the measurement was individualised for every participant and every condition. On the other hand, for P3b and slow wave, a simple average within the common time interval was calculated, since both peaks are not as focal as P1 and N1.*

STATISTICAL ANALYSIS

Behavioural Data: Accuracy (proportion of correct responses) and reaction times were analysed using a four-way repeated-measures analysis of variance (ANOVA) with the following factors: post-receptoral mechanism (3 levels: luminance-defined, isoluminant bluish and reddish), WM load (one, two or three stimuli to remember), contrast (contrast level at which the stimuli were presented: low or high) and memory probe congruency (match/nonmatch). Post-hoc pairwise comparisons were conducted when the main effect was significant. More complex interactions were decomposed by doing separate repeated measure ANOVAs along the levels of one of the factors. The Greenhouse-Geisser correction was used when required.

ERPs: A 3-way ANOVA was used with the following factors: mechanism, WM load, and contrast level. This was used for these dependent measures (P1, N1, and P3b during encoding and recognition, and slow wave amplitude during maintenance). For recognition, an additional factor (probe congruency: match or mismatch) was included in the ANOVA.

CORRELATIONS

We performed Pearson correlations for components that showed a main effect of WM load in the ANOVAs to examine whether ERPs were associated with WM accuracy at different load levels. Additionally, we performed a repeated measure correlation (Bakdash & Marusich, 2017) to further explore how the relationship between behavioural accuracy and ERP amplitudes changes with increasing WM load at the level of an individual. This technique, introduced by Bland and Altman (1995), is specifically designed to reveal within-participant associations between repeated measures and can complement the traditional correlations by revealing patterns that are obscured by averaging across participants. As we have data for three different WM load levels and two contrast levels for each participant, repeated measures correlation considers these six data points in each participant to assess whether there is a linear relationship between the effect of WM load in behavioural performance, on the one hand, and the effect of load on amplitude, on the other hand. We corrected the obtained p-values using Bonferroni-Holm correction for multiple comparisons (Holm, 1979).

BEHAVIOURAL RESULTS

1.1.1 ACCURACY

Figure 5 shows the proportion of correct responses for every mechanism at different levels of WM load, presented separately for matching and mismatching memory probes and high and low contrast. Accuracy differed significantly between different mechanisms ($F_{(1.53, 32.12)} = 47.28$, $p < .001$, $\eta^2 = 0.69$). It was significantly higher for luminance compared to the bluish ($t(21) = 7.85$, $p < .001$, $d = 1.67$) and reddish stimuli ($t(21) = 5.01$, $p < .001$, $d = 1.07$). Accuracy was also higher for reddish compared to bluish ($t(21) = -6.57$, $p < .001$, $d = 1.40$).

In addition, with the increase in WM load, accuracy decreased ($F(2, 42) = 23$, $p < .001$, $\eta^2 = 0.92$). Accuracy was higher for load 1 than load 2 ($t(21) = 13.2$, $p < .001$, $d = 2.82$) and load 3 ($t(21) = 17.9$, $p < .001$, $d = 3.82$), and load 2 had higher accuracy than load 3 ($t(21) = 11.1$, $p < .001$, $d = 2.35$).

Accuracy was also higher when the memory probe was a mismatch rather than a match ($F(1, 21) = 4.87$, $p = .039$, $\eta^2 = 0.19$). This was further qualified by two interactions: between mechanism and probe congruency ($F(1.55, 32.48) = 4.26$, $p = .032$, $\eta^2 = 0.17$) as well as the three-way interaction between mechanism, WM load and probe congruency ($F(2.82, 59.1) = 3.41$, $p = .026$, $\eta^2 = 0.14$).

Separate ANOVAs for match and mismatch (*Figure 5*, left) showed that differences between mechanisms were most pronounced for mismatch trials at higher WM load levels. More specifically, an interaction between load and mechanism at mismatch ($F(3, 62.85) = 6.35$, $p = .001$, $\eta^2 = 0.23$) suggested that accuracy for trials with luminance-defined shapes at load 3 was higher than both reddish ($t(21) = 5.15$, $p < .001$, $d = 1.10$) and bluish ($t(21) = 7.81$, $p < .001$, $d = 1.67$). At load 2, luminance accuracy was higher than bluish ($t(21) = 5.23$, $p < .001$, $d = 1.11$) but not reddish ($t(21) = 2.80$, $p = .053$, $d = 0.60$). In addition, at load 2, accuracy for bluish was lower than reddish ($t(21) = -3.33$, $p = .019$, $d = 0.71$). At load 1, there were no significant differences between mechanisms.

On the other hand, for match, WM load and mechanism factors did not interact ($F(4, 84) = 0.11$, $p = 0.98$, $\eta^2 = 0$).
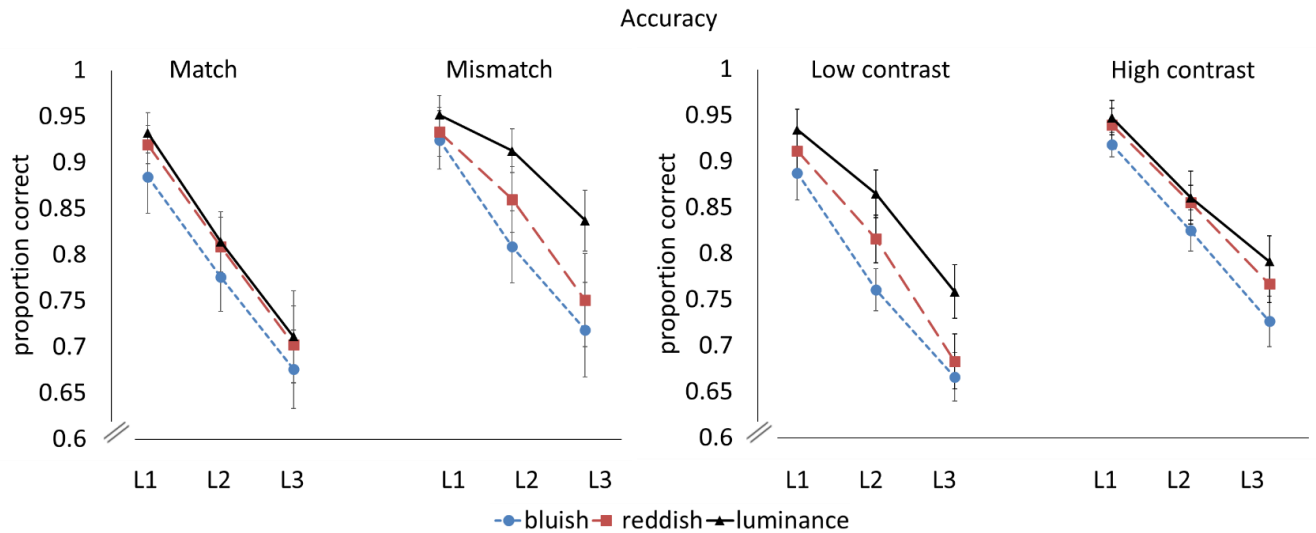
Figure 5. *Proportion of correct responses for the bluish (blue circle), reddish (red square) and luminance stimuli (black triangle) at 3 WM loads shown separately for match and mismatch probes (left) and for low and high contrast stimuli (right). Error bars represent within-subject 95% confidence intervals.*

Stimuli presented at low compared to high contrast were associated with lower performance $(F(1, 21) = 52.42, p < .001, \eta^2 = 0.71$, (*Figure 5*, right). An interaction between mechanism and contrast level was also significant $(F(2, 42) = 4.77, p = .014, \eta^2 = 0.18)$. Differences between different types of stimuli were most pronounced at low contrast and accuracy was better for luminance compared to chromatic stimuli (where all pairwise comparisons were significant; luminance vs. bluish: $t(21) = 7.95, p < .001, d = 1.69$, luminance vs. reddish: $(t(21) = 4.83, p < .001, d = 1.03$, bluish vs. reddish: $t(21) = -3.99, p = .002, d = 0.85)$. At high contrast, accuracy in response to luminance-defined stimuli did not differ from the accuracy in response to reddish shapes $(t(21) = 1.31, p = .20, d = 0.28)$, although, similarly to low contrast, the difference was significant for luminance vs. bluish $(t(21) = 4.08, p = .002, d = 0.87)$ and for bluish vs. reddish $(t(21) = -4.37, p = .001, d = 0.93)$ comparisons.

An interaction between WM load and contrast was also significant $(F(2, 42) = 3.48, p = .040, \eta^2 = 0.14)$. Post-hoc tests confirmed that accuracy at each WM load was higher at high compared to low contrast (all pairwise comparisons significant at $p < .001$).

REACTION TIMES

Figure 6 depicts mean of median reaction times in response to bluish, reddish and luminance shapes. A main effect of mechanism ($F_{(2, 42)} = 23.94$, $p < 0.001$, $\eta^2 = 0.53$) confirmed that RTs were significantly faster in response to luminance-defined stimuli compared to bluish ($t_{(21)} = 6.51$, $p < .001$, $d = 1.39$) and reddish stimuli ($t_{(21)} = -5.32$, $p < .001$, $d = 1.13$). In addition, RTs were also modulated by WM load ($F_{(1.43, 29.92)} = 36.95$, $p < .001$, $\eta^2 = 0.64$) - RTs became slower with increasing WM load (load 1 vs. load 2: $t_{(21)} = -6.26$, $p < .001$, $d = 1.33$, load 2 vs. load 3: $t_{(21)} = -4.65$, $p < .001$, $d = 0.99$).
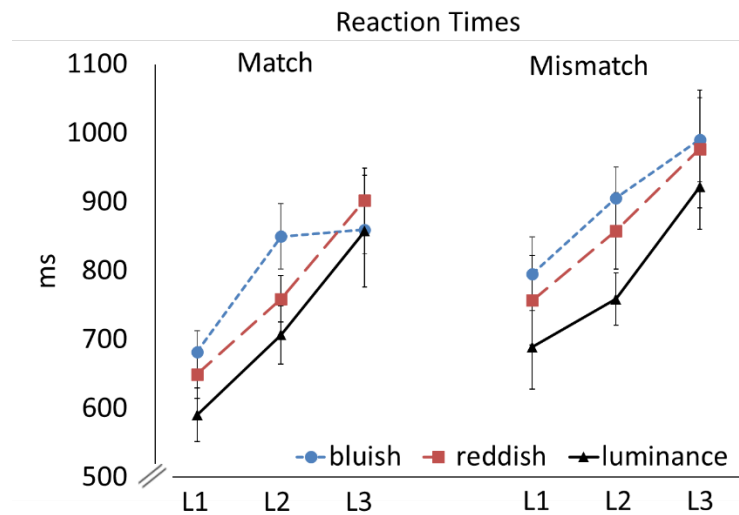

Figure 6. *Reaction times for the bluish (blue circle), reddish (red square) and luminance (black triangle) stimuli at 3 WM loads are shown separately for a match (left) and mismatch (right). Error bars represent within-subject 95% confidence intervals.*

There was also a significant interaction between mechanism and WM load ($F_{(2.25, 47.08)} = 3.81$, $p = .025$, $\eta^2 = 0.15$). Responses to luminance-defined shapes at load 1 were faster than both bluish ($t_{(21)} = -6.44$, $p < .001$, $d = 1.37$) and reddish stimuli ($t_{(21)} = -3.06$, $p = .036$, $d = 0.65$). The same was the case at load 2 (luminance vs. bluish: $t_{(21)} = -4.75$, $p = .001$, $d = 1.01$, vs. reddish: $t_{(21)} = -4.8$, $p = .001$, $d = 1.02$), but not at load 3.

Responses were faster for stimuli presented at high contrast than at low contrast ($F(1, 21)$ = 51.94, p = .001, η^2 = 0.71). Reaction times were also faster when the memory probe matched the remembered stimuli ($F(1, 21)$ = 10.88, p = .004, η^2 = 0.34).

ERP RESULTS

ERP waveforms are presented in *Figure 7* and *Figure 8*.

P1 ENCODING

The P1 component was most pronounced at the 80 – 160 ms time window at electrodes PO7 and PO8. For luminance-defined stimuli, the average onset latency was 68 ms (*SD*: 27 ms). As expected, a distinctive P1 was not observed for isoluminant stimuli.

We obtained a main effect of mechanism ($F(1.50, 31.48)$ = 21.07, p < .001, η^2 = .50). Post-hoc, Bonferroni-corrected tests showed that luminance elicited a greater P1 amplitude than both bluish ($t(31)$ = 5.3, p < .001, d = 0.94) and reddish stimuli ($t(31)$ = 4.5, p < 0.001, d = 0.79). Hence, as predicted, encoding of luminance-defined shapes elicited robust P1 amplitude, while this ERP was absent for bluish and reddish shapes (see Figure 7 C and D), a pattern consistently shown in the literature (Berninger et al., 1989; Martinovic et al., 2011; Murray, Parry, Carden, & Kulikowski, 1986; Tobimatsu, Tomoda, & Kato, 1995, 1996). Importantly, we obtained a significant interaction between WM load and stimulus type ($F(4, 84)$ = 3.96, p = .005, η^2 = .16). P1 amplitude in response to luminance stimuli was modulated by WM load ($F(2, 42)$ = 5.08, p = .011, η^2 = 0.19; see Figure 7 A and B). The amplitude at load 3 was higher than at load 1 ($t(21)$ = 2.87, p = .027, d = 0.61). P1 was also higher for high compared to low contrast stimuli ($F(1, 21)$ = 11.36, p = .003, η^2 = 0.35). In comparison, the P1 amplitude for the bluish and reddish stimuli did not differ significantly with WM load and with contrast.

P1 amplitude

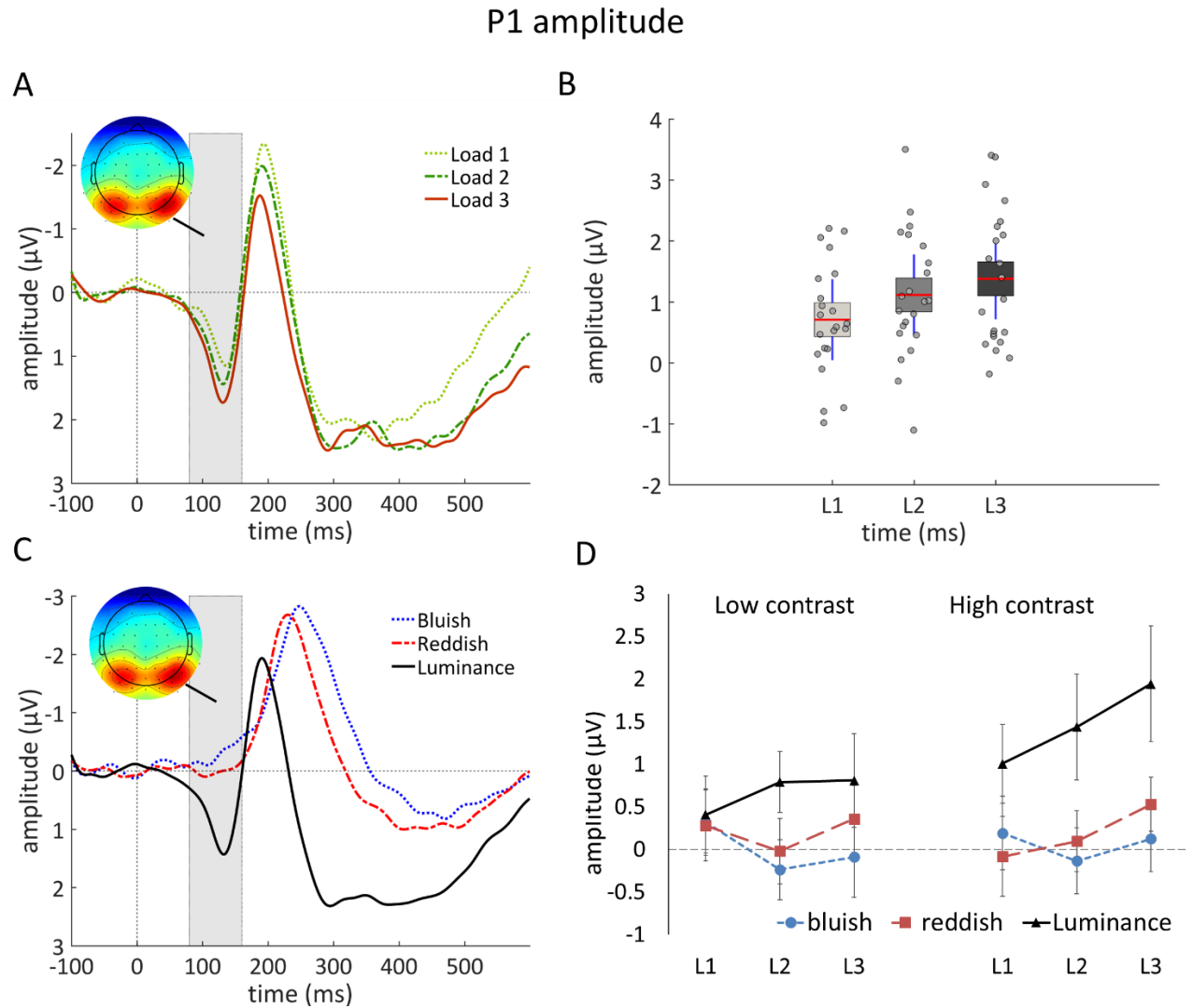**Figure 7. A)** *P1 across electrodes PO7 and PO8 during encoding of luminance-defined stimuli, shown separately for WM load 1, 2 and 3. The shaded box shows the time window of interest (80 – 160 ms). Topography insert depicts average activity in the time window of interest, averaged across all experimental conditions.* **B)** *box plots showing P1 amplitude at every WM load. Red lines inside box plots represent the mean, coloured patches are within-subject 95% confidence intervals, the blue vertical line is one standard deviation, and the dots represent individual average P1 amplitudes for each participant.* **C)** *P1 across electrodes PO7 and PO8 for all WM load and contrast levels, shown separately for mechanisms (bluish, reddish, luminance). Note the lack of a P1 component (80-160 ms time window, shaded area) in response to bluish and reddish stimuli.* **D)** *Line plot of the P1 amplitudes in all experimental conditions, with within-subject confidence intervals.*

N1 ENCODING EFFECTS

The N1 component was most pronounced within the 130 – 300 ms time window at electrodes O1, O2 and Oz. The onset latency for component N1 during encoding was 171 ms (*SD*: 22) for luminance, 194 ms (*SD*: 21.3) for the reddish stimuli and was 188 ms (*SD*: 21) for the bluish stimuli (see *Figure 8* A).

The N1 amplitude differed significantly between the mechanisms ($F(1.34, 28.04) = 14.68$, $p = .001$, $\eta^2 = 0.41$). Luminance stimuli elicited smaller (less negative) N1 amplitudes than both bluish ($t(21) = 4.34$, $p < .001$, $d = 0.93$) and reddish stimuli ($t(21) = 3.76$, $p = .002$, $d = 0.80$). N1 was not, however, modulated by WM load ($F(1.58, 33) = 2.68$, $p = .096$, $\eta^2 = 0.11$). N1 amplitude was higher in response to high compared to low contrast stimuli ($F(1, 21) = 14.72$, $p = .001$, $\eta^2 = 0.41$). An interaction between contrast and WM load was significant ($F(1.71, 35.71) = 3.94$, $p = .035$, $\eta^2 = 0.16$); post-hoc tests indicated that load 1 amplitude at high contrast was higher (i.e. more negative) than at low contrast ($t(21) = -3.63$, $p = .018$, $d = 0.77$).

P3B ENCODING EFFECTS

The P3b component was most pronounced within the 200 – 1000 ms time window at electrodes CP1, CP2, CPz, P1, P2, and Pz (see *Figure 8* B).

The mean P3b amplitude did not differ significantly between mechanisms ($F(2, 42) = 0.03$, $p = .98$, $\eta^2 = 0$) and there was no interaction between mechanism and WM load ($F(4, 84) = 0.32$, $p = .65$, $\eta^2 = 0.03$). The amplitude was modulated by WM load ($F(1.15, 24.1) = 9.28$, $p = .005$, $\eta^2 = 0.31$). Load 1 had a greater amplitude than load 2 ($t(21) = 3.49$, $p = .006$, $d = 0.74$) and load 3 ($t(21) = 2.73$, $p = .024$, $d = 0.58$). Load 2 was not significantly different from load 3 ($t(21) = -1.57$, $p = .13$, $d = 0.33$). Main effect of contrast was not significant ($F(1,21) = 2.19$, $p = .15$, $\eta^2 = 0.09$). No interactions were significant.
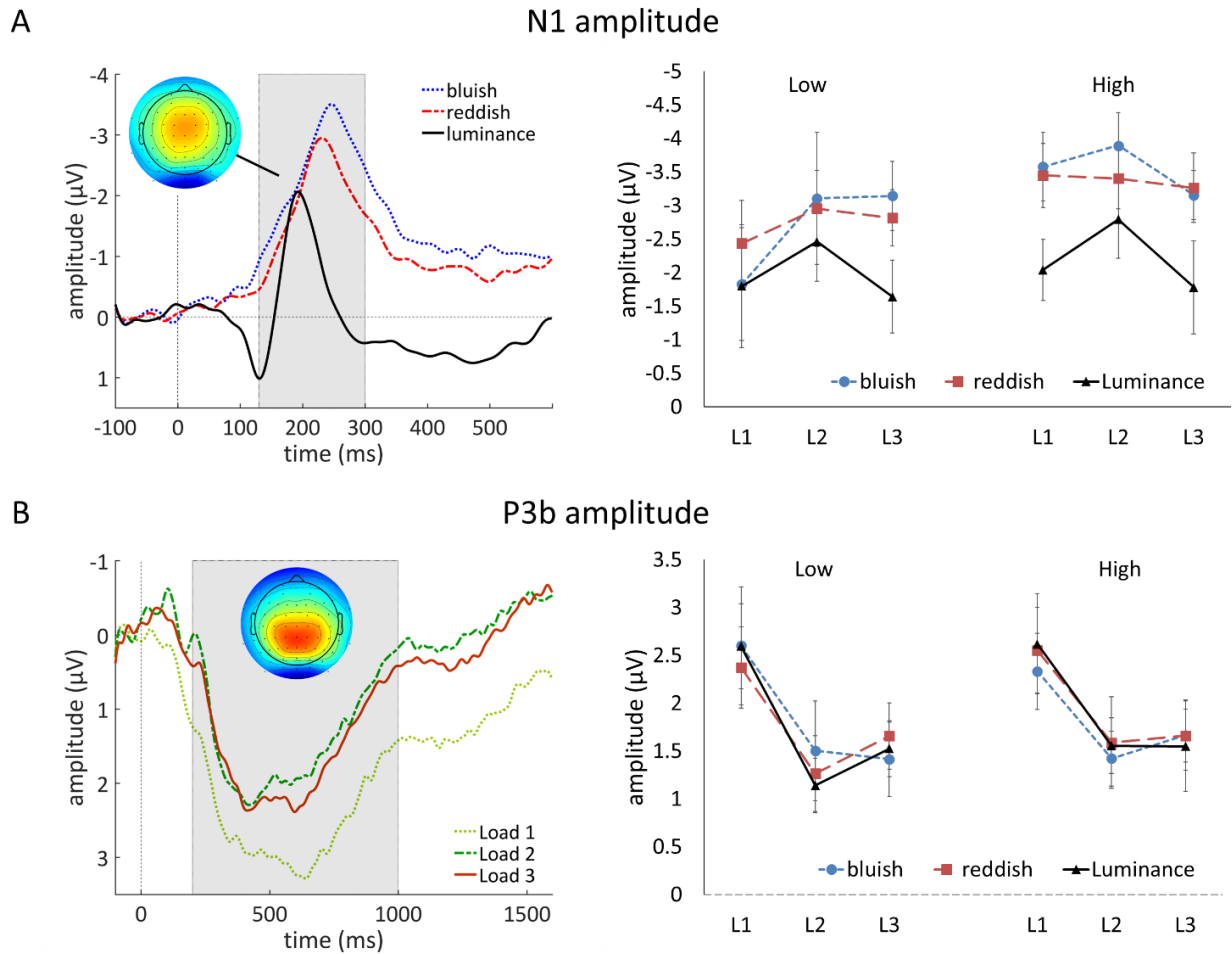
Figure 8 *ERP waveforms (left column) and line plots of ERP amplitudes (right column).* ***A)*** *N1 (average of electrodes O1, O2, and Oz) for the main effect of mechanism and line plot of N1 amplitudes for all stimuli types, WM load and two contrast levels* ***B)*** *P3b (average of electrodes CP1/2/z and P1/2/z) for the main effect of WM load and Line plot of P3b amplitudes for all stimuli types, WM load and two contrast levels. Grey-shaded areas show analysis time-window, and topography inserts represent activity within that area across the scalp averaged across all experimental conditions. The dashed line at 600ms in the slow wave ERP plot corresponds to stimulus offset. Error bars in the line plots are within-subject confidence intervals.*

MAINTENANCE AND RECOGNITION

While we did find effects that are consistent with the previous literature (for example, occipital slow wave amplitude was modulated by WM load; Luria et al., 2016), none of the effects during maintenance or recognition stages pointed to the differential contribution of either luminance or chromatic signals to WM. Full results (main effects and interactions) are presented in Table 2.

Table 2 *Main effects for ERPs during maintenance and recognition stages. Significant effects are marked in bold and p-values lower than .05 are underlined. Note that for P1 during recognition, only the luminance mechanism was subjected to analysis, given that the P1 was not elicited for bluish and reddish stimuli, which was also the case during the encoding stage.*

WM stage	ERP	Effect	F (df)	p-value	η²
Maintenance	Slow wave	Mechanism	0.98 (2, 42)	0.38	0.04
		WM load	**18.28 (1.35, 28.30)†**	**< .001**	**0.46**
		Contrast level	.95 (1, 21)	0.34	0.04
Recognition	P1	Mechanism	N/A		
		WM load	1.65 (2, 42)	0.2	0.07
		Contrast level	3.14 (1, 21)	0.091	0.13
		Probe	0.20 (1, 21)	0.66	0.01
	N1	**Mechanism**	**14.2 (1.47, 30.8)†**	**< .001**	**0.4**
		WM load	0.21 (2, 42)	0.81	0.01
		Contrast level	**8.23 (1, 21)**	**0.009**	**0.28**
		Probe	0.73 (1, 21)	0.4	0.03
	P3b	**Mechanism**	**4.17 (2, 42)**	**0.022**	**0.17**
		WM load	**9.98 (1.39, 29.26)†**	**0.002**	**0.32**
		Contrast level	**11.48 (1, 21)**	**0.003**	**0.35**
		Probe	0.42 (1, 21)	0.52	0.02

† = Greenhouse-Geisser correction applied

CORRELATIONS

We first used Pearson correlation to examine the relationship between ERP amplitudes and WM accuracy for components where a main effect of WM load was detected with an ANOVA (i.e. P1 luminance only and collapsed across mechanisms for P3b at encoding, slow wave during the maintenance, and P3b during recognition). We found a significant correlation for P1 luminance at load 3 ($r = .62$, $p = .027$;), but not load 1 and load 2 (see *Figure 9*). Full results are presented in *Table 3*.
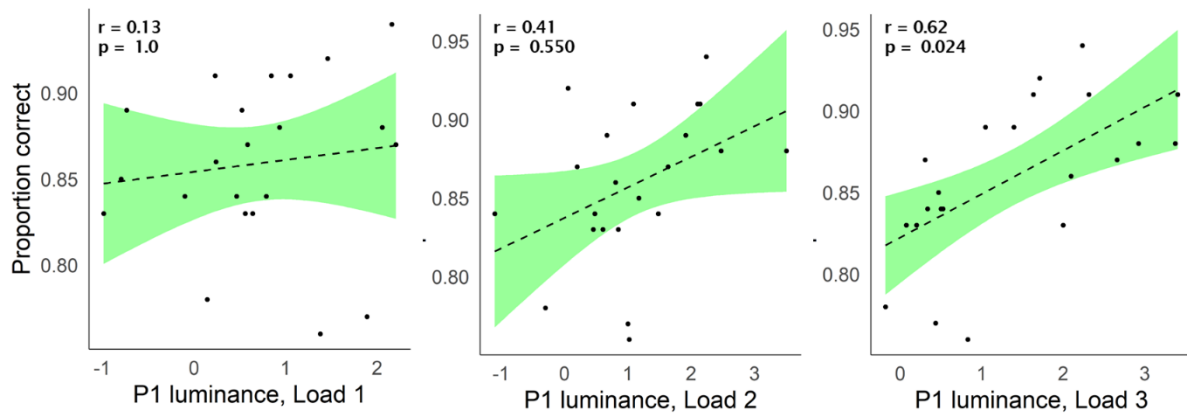
Figure 9 *Correlation between the proportion of correct responses in the luminance condition with P1 luminance amplitudes at load 1 (left), 2 (middle), and 3 (right).*

Table 3 *Correlations between behavioural performance and ERP components for which the main effect of load was significant in the ANOVA. The table includes correlation coefficients, unadjusted p-values, and p-values adjusted for multiple comparisons using Bonferroni-Holm correction (12 comparisons). Significant effects are shown in bold and underlined.*

	P1 encoding (luminance)			P3b encoding		
	r	p-value	p (Bon.-Holm)	r	p-value	p (Bon.-Holm)
Load 1	0.13	0.56	1	0.46	0.03	0.33
Load 2	0.41	0.055	0.55	0.32	0.14	1
Load 3	**0.62**	**0.002**	**0.027**	0.20	0.38	1

	Slow wave			P3b recognition		
	r	p-value	p (Bon.-Holm)	r	p-value	p (Bon.-Holm)
Load 1	-0.01	0.98	1	0.31	0.16	1
Load 2	0.23	0.30	1	0.32	0.15	1
Load 3	0.41	0.06	0.55	0.33	0.13	1

Additionally, for the ERP components above, we performed a repeated measure correlation (Bakdash& Marusich, 2017) between amplitude and accuracy to explore if the effect of load in ERPs and behavioural performance is consistent across participants (see *Figure 10*). Here, the intra-individual P1 amplitudes correlated negatively with behavioural accuracy: lower amplitudes were associated with better behavioural performance (R_{rm} = -0.21, p = .027; see *Figure 10*). Note that the P1 amplitude tended to be lower for load 1; the behavioural performance tended to be better for this load level as well. Taken together, the

repeated measure correlation confirms that the relation between P1 and accuracy is robust across all participants. The analysis also showed significant correlations between P3b during encoding, the slow wave and for the P3b during recognition for all stimuli types. Full results are presented in *Table 4*.

Table 4 Repeated measures correlation coefficients (Rrm) and the corresponding p-values for correlations between behavioural performance and ERP components, shown for each mechanism, during encoding, maintenance, and recognition. The table includes correlation coefficients, uncorrected p-values, and p-values adjusted for multiple comparisons using Bonferroni-Holm correction (10 comparisons). Significant effects are shown in bold and underlined.

	Bluish			Reddish			Luminance		
	Rrm	p-value	p (Bon.-Holm)	Rrm	p-value	p (Bon.-Holm)	Rrm	p-value	p (Bon.-Holm)
P1	N/A						-0.21	0.025	0.027
P3B	0.37	< .001	< .001	0.23	0.014	0.027	0.26	0.005	0.021
Slow Wave	-0.45	< .001	< .001	-0.59	< .001	< .001	-0.46	< .001	< .001
P3b (recognition)	0.42	< .001	< .001	0.27	0.004	0.02	0.25	0.009	0.027

To explore the possibility that P1 amplitude during encoding is linked to slow wave during the maintenance, we additionally examined the relationship between the P1 and slow wave amplitude using a repeated measures correlation approach. We found a positive correlation; the higher the P1 amplitude, the higher the slow wave amplitude (r_{rm} = .22, p = .019).
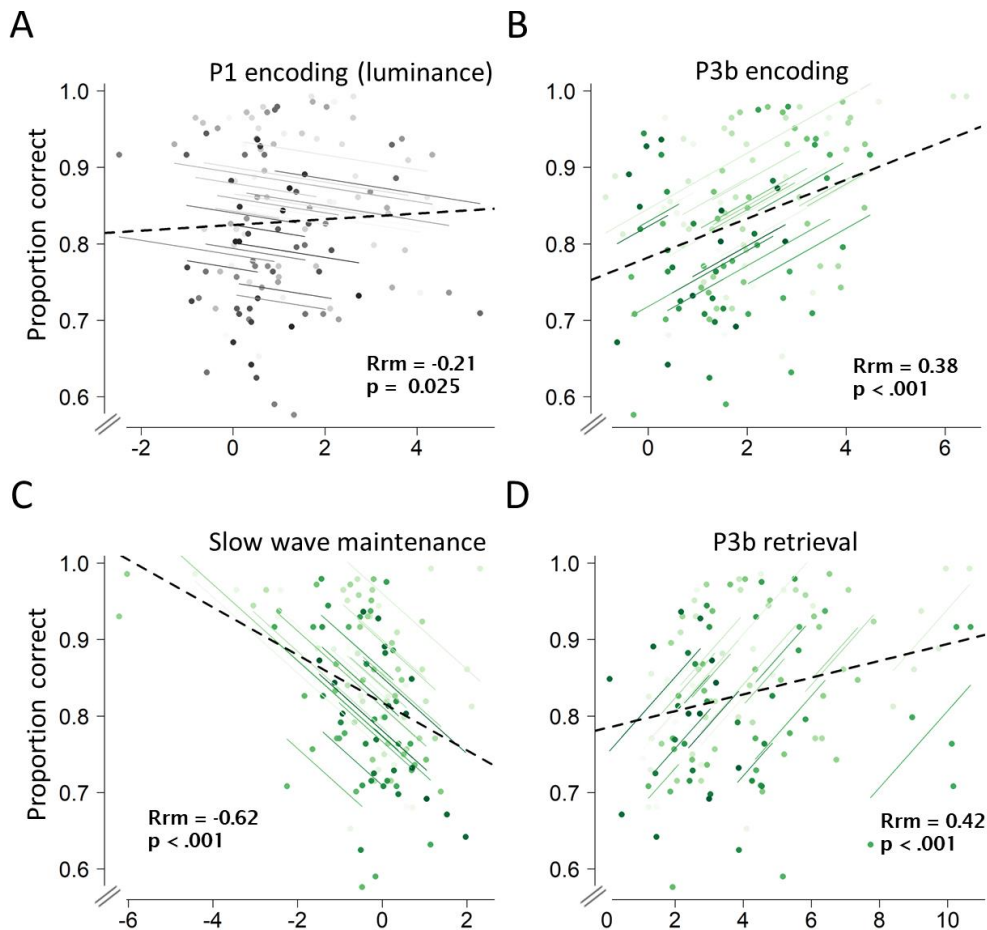
Figure 10 *Repeated measures correlation plots between ERP amplitudes and proportion of correct responses for A) P1 in response to Luminance B) P3b (averaged over stimuli types) C) Slow wave (averaged over stimuli types) D) P3b during recognition stage (averaged over stimuli types). Each data point represents trial-averaged data of one participant (6 data points per participant, corresponding to three levels of WM load and two contrast levels; the figure uses a single shade per participant). P-values are adjusted for multiple comparisons using Bonferroni-Holm correction.*

DISCUSSION

We examined if luminance signals are more efficient than chromatic signals in driving the encoding into WM representations. In two experiments, we confirmed that working memory interacts with perceptual processing and showed for the first time that this process was mediated predominantly by luminance inputs. Our results provide evidence for a direct connection between low-level perceptual mechanisms and WM by showing a crucial role of luminance in forming WM representations and supporting WM recognition. This is in agreement with a recent study (Constant & Liesefeld, 2021) which showed that the salience of WM representations affects task performance. Here we show that luminance during

encoding contributes to the strength of stimulus representation, as indicated by the more efficient processing of luminance contrast in the delayed recognition task and higher early amplitude in the EEG.

Great care was taken to exclude the possibility that the results are due to mere saliency differences between luminance and colour-defined stimuli. In our psychophysics experiment, contrasts are expressed in detection threshold units. In our EEG experiment, we adopt a similar approach and equate the contrast of stimuli for each participant using a shape discrimination threshold task. To achieve a good signal-to-noise ratio in the EEG, these contrasts were then scaled up. The relative differences between contrast levels in discrimination threshold units were thus maintained. Our data suggests that these procedures were successful, as the pattern of results for luminance and colour differed for trials with matching and mismatching memory probes (see e.g. Martinovic et al., 2011 and Kosilo et al., 2013 for an analogous dissociation in an object classification task). The fact that we present a similar pattern of results across two separate experiments that rely on different methods (psychophysics, behavioural accuracy, ERPs) further strengthens our conclusion of the special role of luminance contrast in WM performance.

WM performance was better for luminance-defined compared to isoluminant shapes. While WM performance decreased with increasing WM load for all stimuli, at higher loads WM performance was noticeably better sustained for luminance-defined shapes. This pattern was observed both from reduced WM thresholds in Exp. 1 and higher accuracy in the delayed recognition task (Exp.2). Hence, luminance influenced WM performance. The EEG correlates of perceptual processing were highly consistent with these behavioural effects. As mentioned in the introduction, visual components P1 and N1 served as differential indices of early stimulus encoding: P1 for luminance and N1 for chromatic mechanisms. Our results demonstrated that the P1 in response to luminance-defined shapes was modulated by WM load during encoding. This was not the case for the N1 in response to chromatic shapes. In addition, at load 3, the luminance P1 was correlated with accuracy. The repeated measures

correlation confirmed that the relation between P1 and accuracy was robust across all observers. It showed that on an individual level, the P1 amplitude decreased with increasing WM load, reflecting the drop in accuracy with higher WM load in the behavioural data. However, across the sample, those participants who had higher P1 amplitudes also showed better performance. The processing stages indexed by the P1 component have been shown to be important for successful encoding (Haenschel et al., 2007). Here we show, for the first time, that this WM influence on P1 is driven by luminance contrast. The later ERP components, P3b during encoding and the slow wave during maintenance, were also modulated by WM load, but not by the visual mechanism. ERP amplitudes during the processing of the memory probe, i.e. during the recognition stage, also failed to show effects that would point to a mechanism-dependent WM engagement. This suggests that these interactions are most important early on, during the formation of the representation.

A candidate route through which luminance contrast exerts its effect on WM processing is that it allows for a more precise and thus more efficient formation of the representation, resulting in a better signal-to-noise ratio at encoding. The luminance advantage might be explained through less efficient isoluminant signals, which (on their own) cannot sufficiently support adequate shape encoding. This interpretation is also consistent with our finding that, at low contrast, accuracy was higher for luminance compared to chromatic stimuli, while at high contrast the accuracy difference between the mechanisms was not prominent. The advantage of a more robust luminance signal can be readily observed at low contrast, while at high contrast, the efficiency difference between mechanisms will be less pronounced.

Our results show that differences in performance between luminance and colour-defined stimuli are especially pronounced at higher WM loads and at low contrast. We argue that the WM system is more efficient in processing luminance-defined stimuli due to better fidelity and reduced noise. It has been argued (Bays, 2014; Bays et al., 2011) that increasing the number of stimuli held in memory increases the neural noise, and that such noise is the main source of errors in WM. It is also evident that the neural noise accumulates over time, also

contributing to less precise working memory representations, and thus leading to errors (Salmela, Lahde, & Saarinen, 2012). In line with this, there is also evidence that prolonging the maintenance period has a negative effect on discrimination performance (Najima, Dosher, Chu, & Lu, 2011; Salmela et al., 2012; Wilken & Ma, 2004) as the representation of the majority of visual features (such as orientation or contrast) decays over time (Pasternak & Greenlee, 2005). 2012). As Bays (2014) argues, neural noise is the main culprit behind errors in WM. The result from our psychophysical experiment would support this: lower WM thresholds at higher loads for luminance-defined items would imply more efficient processing of the stimuli and higher precision of the stored representations. This might benefit initial stimulus formation during encoding, which may help to sustain the representation during the maintenance and facilitate the comparison between the probe and the stimuli held in memory.

The decoded strength of WM representations in the early visual cortex is strongly correlated with behavioural performance (Iamshchinina et al., 2021). In addition, Rademaker, Chunharas and Serences (2019) show that salient visual distractors decrease the precision of WM representations. From this, they proposed that sensory areas form a "comparison circuit", and that the early visual cortex is necessary to sustain high-fidelity memories. It is conceivable that given better fidelity of shape-encoding achieved through luminance projections, the representation is stronger and comparison will be easier, and thus performance better. Indeed, an explorative, correlational analysis supported this interpretation by showing that the higher the P1 amplitude, the higher the slow wave amplitude. This may suggest that the stability of the initially formed representation helps maintain the stimulus during maintenance. Future studies can explore this possibility more directly, for example by looking at whether stronger representation provides better protection from interference.

During the memory recognition phase, participants had to decide whether a stimulus matched or did not match the stimuli held in memory. Comparing behavioural accuracy

between match and mismatch stimuli showed that performance was better in response to mismatching memory probes when they were defined by luminance contrast at higher WM loads. This suggests that luminance-driven inputs help to flag the difference between the stimuli during memory-probe comparison. These differences suggest that match and mismatch appear to be tapping into different recognition processes which might impact performance differently (see e.g., Johnson et al., 2009 for a theoretical model of same/different judgements in WM task or Bledowski et al., 2011). Our finding that luminance facilitated accurate rejection of mismatched probes is worth exploring in future studies to uncover the underlying template-matching mechanism for which luminance information is particularly beneficial.

Our results are in line with earlier findings from perceptual studies that showed that luminance signals are especially suitable for processing and integration of edges and contours, and thus are important for the perception of form (Beaudot & Mullen, 2005; Gregory & Heard, 1989; Lu & Fender, 1972; Gregory, 1977; Livingstone & Hubel, 1988; Livingstone & Hubel, 1987; Mullen, Beaudot, & McIlhagga, 2000). Other studies also showed that luminance plays a special role in object recognition and discrimination; for example, luminance-defined objects are recognised and distinguished from non-objects faster and more accurately (Bar, 2003; Kveraga et al., 2007; Martinovic et al., 2011).

Our experiments extend these findings into the WM domain: luminance and chromatic channels appear to provide differential contributions to WM for shape, with the luminance information being especially important for WM performance. In the WM domain, it has been shown that performance is facilitated by top-down interactions with frontal areas (see e.g. Gazzaley, 2011). According to Gazzaley (2011), such facilitation would need to be initiated sufficiently early. Such a "head start" could be achieved via fast luminance projections (Bar, 2003). In line with previous studies showing prefrontal facilitation of the P1 (Barcelo, Suwazono, & Knight, 2000, Zanto et al., 2011) the modulation of the early visual component

P1 by luminance-defined stimuli in our experiment might be supported by top-down processes.

CONCLUSION

WM encoding appears to share some of its neural architecture with perception (Harrison, Tong, 2009; Pasternak & Greenlee, 2005). Hence, we investigated whether building a memory representation is governed by analogous processes responsible for building perceptual representations of the visual world. We found that processing of luminance-defined shapes leads to better WM performance when compared to isoluminant shapes. Our study delineates brain-behaviour correlations in early stimulus processing during WM encoding and validates a new approach towards studying visual WM which is informed by colour psychophysics. Overall, our study contributes to the understanding of how sensory signals are transformed into accurate memory representations.

ACKNOWLEDGEMENTS

AUTHOR CONTRIBUTIONS

JM, MK & CH designed the experiments, JM & MK programmed the experiments, MK collected the data, and MK, JM & CH analysed the data and wrote the manuscript.

DATA SHARING

Data and code used in analyses are made available on the Open Science Framework database (https://osf.io/c9qhu/?view_only=8865565691b54ded80f501b2da86e19f).

REFERENCES

Albers, A. M., Kok, P., Toni, I., Dijkerman, H. C., & de Lange, F. P. (2013). Shared

Representations for Working Memory and Mental Imagery in Early Visual Cortex. Current

Biology, 23(15), 1427–1431. https://doi.org/10.1016/j.cub.2013.05.065

Baddeley, A. (2003). Working memory: looking back and looking forward. Nature Reviews.

Neuroscience, 4(10), 829–839. https://doi.org/10.1038/nrn1201

Baddeley, A. (2010). Working memory. *Current Biolog*y, 20(4), R136-40.

https://doi.org/10.1016/j.cub.2009.12.014

Baddeley, A. D., & Hitch, G. (1974). Working Memory. https://doi.org/10.1016/S0079-

7421(08)60452-1

Bakdash, J. Z., & Marusich, L. R. (2017). Repeated measures correlation. *Frontiers in

psychology*, *8*, 456. https://doi.org/10.3389/fpsyg.2017.00456

Baker, D. H., Lygo, F. A., Meese, T. S., & Georgeson, M. A. (2018). Binocular summation

revisited: Beyond √2. *Psychological bulletin*, 144(11), 1186–1199.

https://doi.org/10.1037/bul0000163

Bar, M. (2003). A cortical mechanism for triggering top-down facilitation in visual object

recognition. *Journal of Cognitive Neuroscience*, 15(4), 600–609.

https://doi.org/10.1162/089892903321662976

Barbur, J. L., Rodriguez-Carmona, M., & Harlow, A. J. (2006). Establishing the statistical

limits of "normal" chromatic sensitivity. In *CIE Expert Symposium, CIE Proceedings 75 Years

of the Standard Colorimetric Observer*.

Barcelo, F., Suwazono, S., & Knight, R. T. (2000). Prefrontal modulation of visual processing

in humans. *Nature Neuroscience*, 3(4), 399–404. https://doi.org/10.1038/73975

Bays, P. M. (2014). Noise in Neural Populations Accounts for Errors in Working Memory.

*Journal of Neuroscienc*e, 34(10), 3632–3645. https://doi.org/10.1523/JNEUROSCI.3204-

13.2014

Bays, P. M., Gorgoraptis, N., Wee, N., Marshall, L., Husain, M., & S., K. J. (2011). Temporal

dynamics of encoding, storage, and reallocation of visual working memory. Journal of Vision, 11(10), 6–6. https://doi.org/10.1167/11.10.6

Beaudot, W. H. a, & Mullen, K. T. (2005). Orientation selectivity in luminance and color vision assessed using 2-d band-pass filtered spatial noise. *Vision Research,* 45(6), 687–696. https://doi.org/10.1016/j.visres.2004.09.023

Berggren, N., & Eimer, M. (2016). Does Contralateral Delay Activity Reflect Working Memory Storage or the Current Focus of Spatial Attention within Visual Working Memory? *Journal of cognitive neuroscience*, 28(12), 2003–2020. https://doi.org/10.1162/jocn_a_01019

Berninger, T. A., Arden, G. B., Hogg, C. R., & Frumkes, T. (1989). Separable evoked retinal and cortical potentials from each major visual pathway: preliminary results. *British Journal of Ophthalmology*, 73(7), 502–511. https://doi.org/10.1136/bjo.73.7.502

Bittner, R. A., Linden, D. E. J., Roebroeck, A., Härtling, F., Rotarska-Jagiela, A., Maurer, K., … Haenschel, C. (2015). The When and Where of Working Memory Dysfunction in Early-Onset Schizophrenia—A Functional Magnetic Resonance Imaging Study. *Cerebral Cortex*, 25(9), 2494–2506. https://doi.org/10.1093/cercor/bhu050

Bland, J. M., & Altman, D. G. (1995). Statistics notes: Calculating correlation coefficients with repeated observations: Part 1—correlation within subjects. *Bmj*, *310*(6977), 446. https://doi.org/10.1136/bmj.310.6977.446

Bledowski, C., Cohen Kadosh, K., Wibral, M., Rahm, B., Bittner, R. A., Hoechstetter, K., … Linden, D. E. J. (2006). Mental Chronometry of Working Memory Retrieval: A Combined Functional Magnetic Resonance Imaging and Event-Related Potentials Approach. *Journal of Neuroscience*, 26(3), 821–829. https://doi.org/10.1523/JNEUROSCI.3542-05.2006

Bledowski, C., Kaiser, J., Wibral, M., Yildiz-Erzberger, K., & Rahm, B. (2011). Separable Neural Bases for Subprocesses of Recognition in Working Memory. *Cerebral Cortex*, 1–9. 1991. https://doi.org/10.1093/cercor/bhr276

Bullier, J. (2001). Integrated model of visual processing. Brain Research. Brain Research Reviews, 36(2–3), 96–107. https://doi.org/10.1016/S0165-0173(01)00085-6

Campbell, R. (2020). notBoxPlot (https://github.com/raacampbell/notBoxPlot), GitHub.

Chaumon, M., Bishop, D. V. M., & Busch, N. A. (2015). A practical guide to the selection of independent components of the electroencephalogram for artifact correction. *Journal of Neuroscience Methods*, 250, 47–63. https://doi.org/10.1016/j.jneumeth.2015.02.025

Christophel, T. B., Klink, P. C., Spitzer, B., Roelfsema, P. R., & Haynes, J.-D. (2017). The Distributed Nature of Working Memory. Trends in Cognitive Sciences, 21(2), 111–124. https://doi.org/10.1016/j.tics.2016.12.007

Constant, M., & Liesefeld, H. R. (2021). Massive effects of saliency on information processing in visual working memory. *Psychological Science*, *32*(5), 682-691. https://doi.org/10.1177/0956797620975785

Cousineau, D. (2005). Confidence intervals in within-subject designs: A simpler solution to Loftus and Masson's method. *Tutorials in quantitative methods for psychology*, *1*(1), 42-45.

Crognale, M. A. (2002). Development, maturation, and aging of chromatic visual pathways: VEP results. Journal of Vision, 2(6), 438–450. https://doi.org/10.1167/2.6.2

D'Esposito, M., & Postle, B. R. (2015). The Cognitive Neuroscience of Working Memory. Annual Review of Psychology, 66(1), 115–142. https://doi.org/10.1146/annurev-psych-010814-015031

De Valois, K. K., & Kooi, F. (1991). Functional Classification of Parallel Visual Pathways. In From Pigments to Perception (pp. 165–171). https://doi.org/10.1007/978-1-4615-3718-2_18

Delorme, A., & Makeig, S. (2004). EEGLAB: an open source toolbox for analysis of single-trial EEG dynamics including independent component analysis. *Journal of Neuroscience Methods*, 134(1), 9–21. https://doi.org/10.1016/j.jneumeth.2003.10.009

Derrington, A. M., Krauskopf, J., & Lennie, P. (1984). Chromatic mechanisms in lateral geniculate nucleus of macaque. The Journal of Physiology, 357, 241–265. https://doi.org/10.1113/jphysiol.1984.sp015499

D'Esposito, M., & Postle, B. R. (2015). The cognitive neuroscience of working memory. *Annual review of psychology*, *66*. https://doi.org/10.1146/annurev-psych-010814-015031

Ellemberg, D., & Hammarrenger, B. (2001). Contrast dependency of VEPs as a function of spatial frequency: the parvocellular and magnocellular contributions to human VEPs. *Spatial*

Vision, 15(1), 99–111. https://doi.org/10.1163/15685680152692042

Eriksson, J., Vogel, E. K., Lansner, A., Bergström, F., & Nyberg, L. (2015). Neurocognitive Architecture of Working Memory. Neuron, 88(1), 33–46. https://doi.org/10.1016/j.neuron.2015.09.020

Feldmann-Wüstefeld, T., Vogel, E. K., & Awh, E. (2018). Contralateral Delay Activity Indexes Working Memory Storage, Not the Current Focus of Spatial Attention. *Journal of cognitive neuroscience*, 30(8), 1185–1196. https://doi.org/10.1162/jocn_a_01271

Fukuda, K., & Vogel, E. K. (2009). Human variation in overriding attentional capture. *The Journal of Neuroscience*, 29(27), 8726–8733. https://doi.org/10.1523/JNEUROSCI.2145-09.2009

Gao, T., Gao, Z., Li, J., Sun, Z., & Shen, M. (2011). The perceptual root of object-based storage: An interactive model of perception and visual working memory. Journal of Experimental Psychology: Human Perception and Performance, 37(6), 1803–1823. https://doi.org/10.1037/a0025637

Gazzaley, A. (2011). Influence of early attentional modulation on working memory. *Neuropsychologia*, 49(6), 1410–1424. https://doi.org/10.1016/j.neuropsychologia.2010.12.022

Gazzaley, A., Cooney, J. W., McEvoy, K., Knight, R. T., & D'Esposito, M. (2005). Top-down enhancement and suppression of the magnitude and speed of neural activity. Journal of *Cognitive Neuroscience*, 17(3), 507–517. https://doi.org/10.1162/0898929053279522

Gegenfurtner, K. R., & Rieger, J. (2000). Sensory and cognitive contributions of color to the recognition of natural scenes. Current Biology, 10(13), 805–808. https://doi.org/10.1016/S0960-9822(00)00563-7

Gegenfurtner, K. R., & Kiper, D. C. (2003). Color vision. 181–206. https://doi.org/10.1146/annurev.neuro.26.041002.131116

Gerth, C., Delahunt, P. B., Crognale, M. A., & Werner, J. S. (2003). Topography of the chromatic pattern-onset VEP. Journal of Vision, 3(2), 171–182. https://doi.org/10.1167/3.2.5

Gregory, R. L. (1977). Vision with Isoluminant Colour Contrast: 1. A Projection Technique

and Observations. *Perception*, 6(1), 113–119. https://doi.org/10.1068/p060113

Gregory, R. L., & Heard, P. (1989). Some phenomena and implications of isoluminance. *Seeing contours and colour*, 725.

Grinter, E. J., Maybery, M. T., & Badcock, D. R. (2010). Vision in developmental disorders: Is there a dorsal stream deficit? Brain Research Bulletin, 82(3–4), 147–160. https://doi.org/10.1016/j.brainresbull.2010.02.016

Haenschel, C., Bittner, R. A, Haertling, F., Rotarska-Jagiela, A., Maurer, K., Singer, W., & Linden, D. E. J. (2007). Contribution of impaired early-stage visual processing to working memory dysfunction in adolescents with schizophrenia: a study with event-related potentials and functional magnetic resonance imaging. *Archives of General Psychiatry*, 64(11), 1229–1240. https://doi.org/10.1001/archpsyc.64.11.1229

Handy, T. C., & Mangun, G. R. (2000). Attention and spatial selection: Electrophysiological evidence for modulation by perceptual load. Perception & Psychophysics, 62(1), 175–186. https://doi.org/10.3758/BF03212070

Hardman, A. C., & Martinovic, J. (2021). Salience of spatiochromatic patterns. *Journal of Vision*, *21*(4), 7-7. https://doi.org/10.1167/jov.21.4.7

Hardman, A., Töllner, T., & Martinovic, J. (2020). Neural differences between chromatic-and luminance-driven attentional salience in visual search. *Journal of vision*, *20*(3), 5-5. https://doi.org/10.1167/jovi.20.3.5

Harrison, W. J., & Bays, P. M. (2018). Visual working memory is independent of the cortical spacing between memoranda. *Journal of Neuroscience*, *38*(12), 3116-3123. https://doi.org/10.1523/JNEUROSCI.2645-17.2017

Harrison, S.A., & Tong, F. (2009). Decoding reveals the contents of visual working memory in early visual areas. Nature, 458(7238), 632–635. https://doi.org/10.1038/nature07832.Decoding

Hicks, T. P., Lee, B. B., & Vidyasagar, T. R. (1983). The responses of cells in macaque lateral geniculate nucleus to sinusoidal gratings. *The Journal of Physiology*, 337(1), 183–200. https://doi.org/10.1113/jphysiol.1983.sp014619

Hillyard, S. A., Vogel, E. K., & Luck, S. J. (1998). Sensory gain control (amplification) as a mechanism of selective attention: electrophysiological and neuroimaging evidence. *Philosophical Transactions of the Royal Society of London. Series B, Biological Sciences*, 353(1373), 1257–1270. https://doi.org/10.1098/rstb.1998.0281

Holm, S. (1979). A simple sequentially rejective multiple test procedure. *Scandinavian journal of statistics*, 65-70. https://www.jstor.org/stable/4615733

Hyun, J., Woodman, G., & Vogel, E. (2009). The comparison of visual working memory representations with perceptual inputs. *Human Perception*, 35(4), 1140–1160. https://doi.org/10.1037/a0015019

Iamshchinina, P., Christophel, T. B., Gayet, S., & Rademaker, R. L. (2021). Essential considerations for exploring visual working memory storage in the human brain. *Visual Cognition*, 1-12. https://doi.org/10.1080/13506285.2021.1915902

Ivanov, I. V, & Mullen, K. T. (2012). The role of local features in shape discrimination of contour- and surface-defined radial frequency patterns at low contrast. *Vision Research*, 52(1), 1–10. https://doi.org/10.1016/j.visres.2011.10.002

Jennings, B. J., & Martinovic, J. (2014). Luminance and color inputs to mid-level and high-level vision. *Journal of Vision*, *14*(2), 9-9. https://doi.org/10.1167/14.2.9

Jennings, B. J., & Martinovic, J. (2015). Chromatic contrast in luminance-defined images affects performance and neural activity during a shape classification task. *Journal of Vision*, 15(15), 21. https://doi.org/10.1167/15.15.21

Johannes, S., Münte, T. F., Heinze, H. J., & Mangun, G. R. (1995). Luminance and spatial attention effects on early visual processing. *Cognitive Brain Research*, 2(3), 189–205. https://doi.org/10.1016/0926-6410(95)90008-X

Kaplan, E., & Shapley, R. M. (1982). X and Y cells in the lateral geniculate nucleus of macaque monkeys. *The Journal of Physiology*, 330(1), 125–143. https://doi.org/10.1113/jphysiol.1982.sp014333

Katus, T., Grubert, A., & Eimer, M. (2015). Electrophysiological Evidence for a Sensory Recruitment Model of Somatosensory Working Memory. *Cerebral Cortex*, 25(12), 4697–

4703. https://doi.org/10.1093/cercor/bhu153

Kiesel, A., Miller, J., Jolicœur, P., & Brisson, B. (2008). Measurement of ERP latency differences: A comparison of single-participant and jackknife-based scoring methods. *Psychophysiology*, 45(2), 250–274. https://doi.org/10.1111/j.1469-8986.2007.00618.x

Kingdom, F. A., & Mullen, K. T. (1995). Separating colour and luminance information in the visual system. *Spatial vision*, *9*(2), 191–219. https://doi.org/10.1163/156856895x00188

Kok, A. (2001). On the utility of P3 amplitude as a measure of processing capacity. *Psychophysiology*, 38(3), 557–577. https://doi.org/10.1016/S0167-8760(98)90168-4

Kosilo, M., Wuerger, S. M., Craddock, M., Jennings, B. J., Hunt, A. R., & Martinovic, J. (2013). Low-level and high-level modulations of fixational saccades and high frequency oscillatory brain activity in a visual object classification task. *Frontiers in psychology*, *4*, 948. https://doi.org/10.3389/fpsyg.2013.00948

Koychev, I., William Deakin, J. F., El-Deredy, W., & Haenschel, C. (2017). Effects of Acute Ketamine Infusion on Visual Working Memory: Event-Related Potentials. Biological Psychiatry: Cognitive *Neuroscience and Neuroimaging*, 2(3), 253–262. https://doi.org/10.1016/j.bpsc.2016.09.008

Kulikowski, J. J. (1976). Effective contrast constancy and linearity of contrast sensation. Vision research, 16(12), 1419-1431. https://doi.org/10.1016/0042-6989(76)90161-9

Kveraga, K., Boshyan, J., & Bar, M. (2007). Magnocellular projections as the trigger of top-down facilitation in recognition. *The Journal of Neuroscience*, 27(48), 13232–13240. https://doi.org/10.1523/JNEUROSCI.3481-07.2007

Lakens, D. (2021, January 4). Sample Size Justification. https://doi.org/10.31234/osf.io/9d3yf

Lara, A. H., & Wallis, J. D. (2015). The Role of Prefrontal Cortex in Working Memory: A Mini Review. Frontiers in Systems Neuroscience, 9, 173. https://doi.org/10.3389/fnsys.2015.00173

Laycock, R., Crewther, D. P., & Crewther, S. G. (2008). The advantage in being magnocellular: a few more remarks on attention and the magnocellular system. Neuroscience and Biobehavioral Reviews, 32(8), 1409–1415.

https://doi.org/10.1016/j.neubiorev.2008.04.008

Laycock, R., Crewther, S. G., & Crewther, D. P. (2007). A role for the "magnocellular advantage" in visual impairments in neurodevelopmental and psychiatric disorders. Neuroscience and Biobehavioral Reviews, 31(3), 363–376. https://doi.org/10.1016/j.neubiorev.2006.10.003

Lee, B. B., & Sun, H. (2009). The chromatic input to cells of the magnocellular pathway of primates. *Journal of Vision*, *9*(2), 15-15. https://doi.org/10.1167/9.2.15

Lehky, S. R. (2000). Deficits in visual feature binding under isoluminant conditions. Journal of *Cognitive Neuroscience*, 12(3), 383–392. https://doi.org/10.1162/089892900562200

Leonards, U., & Singer, W. (1998). Two segmentation mechanisms with differential sensitivity for colour and luminance contrast. *Vision Research*, 38(1), 101–109. https://doi.org/10.1016/S0042-6989(97)00148-X

Linden, D. E. J., Bittner, R. A., Muckli, L., Waltz, J. A., Kriegeskorte, N., Goebel, R., … Munk, M. H. J. (2003). Cortical capacity constraints for visual working memory: dissociation of fMRI load effects in a fronto-parietal network. *NeuroImage*, 20(3), 1518–1530. https://doi.org/10.1016/j.neuroimage.2003.07.021

Livingstone, M., & Hubel, D. (1988). Segregation of form, color, movement, and depth: anatomy, physiology, and perception. *Science*, 240(4853), 740–749. https://doi.org/10.1126/science.3283936

Livingstone, M. S., & Hubel, D. H. (1987). Psychophysical evidence for separate channels for the perception of form, color, movement, and depth. The Journal of Neuroscience : The Official *Journal of the Society for Neuroscience*, 7(11), 3416–3468. https://doi.org/10.1523/JNEUROSCI.07-11-03416.1987

Logie, R. H. (2011). The Functional Organization and Capacity Limits of Working Memory. Current Directions in Psychological Science, 20(4), 240–245. https://doi.org/10.1177/0963721411415340

Lu, C., & Fender, D. H. (1972). The interaction of color and luminance in stereoscopic vision. *Investigative Ophthalmology & Visual Science*, *11*(6), 482-490.

Luck, S. J. (2014). *An introduction to the event-related potential technique*. Cambridge, Mass: MIT Press.

Luck, S. J., & Gaspelin, N. (2017). How to get statistically significant effects in any ERP experiment (and why you shouldn't). *Psychophysiology*, 54(1), 146–157. https://doi.org/10.1111/psyp.12639

Luria, R., Balaban, H., Awh, E., & Vogel, E. K. (2016). The contralateral delay activity as a neural measure of visual working memory. *Neuroscience and Biobehavioral Reviews*, 62, 100–108. https://doi.org/10.1016/j.neubiorev.2016.01.003

Mangun, G.R., Hillyard, S.A., Luck, S.J. (1993) Electrocortical substrates of visual selective attention. In: Attention and performance XIV (Meyer D, Kornblum S, eds), pp 219 –243, Cambridge, MA: MIT.

Martinovic, J. (2016). Magno-, Parvo-, Koniocellular pathways. In M. R. Luo (Ed.). Encyclopedia of color science and technology. New York: Springer. http://dx.doi.org/10.1007/978-1-4419-8071-7_278.

Martinovic, J., Mordal, J., & Wuerger, S. M. (2011). Event-related potentials reveal an early advantage for luminance contours in the processing of objects. *Journal of Vision*, *11*(7), 1-1. https://doi.org/10.1167/11.7.1

Maunsell, J. H., Ghose, G. M., Assad, J. A., McAdams, C. J., Boudreau, C. E., & Noerager, B. D. (n.d.). Visual response latencies of magnocellular and parvocellular LGN neurons in macaque monkeys. *Visual Neuroscience*, 16(1), 1–14. https://doi.org/10.1017/S0952523899156177

McKeefry, D. J., Murray, I. J., & Kulikowski, J. J. (2001). Red--green and blue--yellow mechanisms are matched in sensitivity for temporal and spatial modulation. Vision Research, 41(2), 245–255. https://doi.org/10.1016/S0042-6989(00)00247-9

Morey, R. D. (2008). Confidence Intervals from Normalized Data: A correction to Cousineau (2005). *Tutorials in Quantitative Methods for Psychology*, 4(2), 61–64. https://doi.org/10.20982/tqmp.04.2.p061

Mullen, K. T., Beaudot, W. H., & McIlhagga, W. H. (2000). Contour integration in color vision: a common process for the blue-yellow, red-green and luminance mechanisms? *Vision Research*, 40(6), 639–655. https://doi.org/10.1016/S0042-6989(99)00204-7

Mullen, K. T., & Beaudot, W. H. A. (2002). Comparison of color and luminance vision on a global shape discrimination task. *Vision Research*, 42(5), 565–575. https://doi.org/10.1016/S0042-6989(01)00305-4

Murray I. J., Parry N. R. A., Carden D., Kulikowski J. J. (1986). Human visual evoked-potentials to chromatic and achromatic gratings. *Clinical Vision Sciences*, 1, 231–244.

Najima, R., Dosher, B., Chu, W., & Lu, Z.-L. (2011). Visual working memory performance with contrast and external noise: A load-dependent perceptual template model account. *Journal of Vision*, 11(11), 1254–1254. https://doi.org/10.1167/11.11.1254

Nunez, V., Shapley, R. M., & Gordon, J. (2017). Nonlinear dynamics of cortical responses to color in the human cVEP. *Journal of Vision*, 17(11), 9. https://doi.org/10.1167/17.11.9

Nunez, V., Shapley, R. M., & Gordon, J. (2018). Cortical Double-Opponent Cells in Color Perception: Perceptual Scaling and Chromatic Visual Evoked Potentials. I-Perception, 9(1), 2041669517752715. https://doi.org/10.1177/2041669517752715

Oostenveld, R., Fries, P., Maris, E., & Schoffelen, J.-M. (2011). FieldTrip: Open source software for advanced analysis of MEG, EEG, and invasive electrophysiological data. *Computational Intelligence and Neuroscience,* 2011, 156869. https://doi.org/10.1155/2011/156869

Pajitnov, A. (1984), Tetris [computer software].

Pasternak, T., & Greenlee, M. W. (2005). Working memory in primate sensory systems. *Nature Reviews Neuroscience*, 6(2), 97–107. https://doi.org/10.1038/nrn1603

Phillips, W. (1974). On the distinction between sensory storage and short-term visual memory. *Attention, Perception, & Psychophysics*. https://doi.org/10.3758/BF03203943

Pinal, D., Zurrón, M., Díaz, F., Campbell, W., Bokde, A., & Lai, R. (2015). An Event Related Potentials Study of the Effects of Age, Load and Maintenance Duration on Working Memory Recognition. *Plos One*, 10(11), e0143117. https://doi.org/10.1371/journal.pone.0143117

Poliakov, E., Stokes, M. G., Woolrich, M. W., Mantini, D., & Astle, D. E. (2014). Modulation of alpha power at encoding and retrieval tracks the precision of visual short-term memory. *Journal of neurophysiology*, *112*(11), 2939-2945. https://doi.org/10.1152/jn.00051.2014

Prins, N. & Kingdom, F. A. A. (2018) Applying the Model-Comparison Approach to Test Specific Research Hypotheses in Psychophysical Research Using the Palamedes Toolbox. *Frontiers in Psychology*, 9:1250. https://doi.org/doi: 10.3389/fpsyg.2018.01250

Rademaker, R. L., Chunharas, C., & Serences, J. T. (2019). Coexisting representations of sensory and mnemonic information in human visual cortex. Nature neuroscience, 22(8), 1336-1344. https://doi.org/10.1038/s41593-019-0428-x

R Core Team (2021). R: A language and environment for statistical computing. R Foundation for Statistical Computing, Vienna, Austria. URL https://www.R-project.org/

Ruchkin, D. S., Johnson, R., Canoune, H., & Ritter, W. (1990). Short-term memory storage and retention: an event-related brain potential study. Electroencephalography and Clinical Neurophysiology, 76(5), 419–439. https://doi.org/10.1016/0013-4694(90)90096-3

Ruchkin, D. S., Johnson, R., Grafman, J., Canoune, H., & Ritter, W. (1992). Distinctions and similarities among working memory processes: an event-related potential study. Brain Research. Cognitive Brain Research, 1(1), 53–66. https://doi.org/10.1016/0926-6410(92)90005-C

Ruppertsberg, A. I., Wuerger, S. M., & Bertamini, M. (2003). The chromatic input to global motion perception. *Visual Neuroscience*, 20(4), 421–428. https://doi.org/10.1017/S0952523803204077

Salmela, V. R., Lahde, M., & Saarinen, J. (2012). Visual working memory for amplitude-modulated shapes. *Journal of Vision*, 12(6), 2–2. https://doi.org/10.1167/12.6.2

Scimeca, J. M., Kiyonaga, A., & D'Esposito, M. (2018). Reaffirming the Sensory Recruitment Account of Working Memory. *Trends in cognitive sciences*, *22*(3), 190–192. https://doi.org/10.1016/j.tics.2017.12.007

Schiller, P. H., & Colby, C. L. (1983). The responses of single cells in the lateral geniculate nucleus of the rhesus monkey to color and luminance contrast. *Vision research*, *23*(12),

1631-1641. https://doi.org/10.1016/0042-6989(83)90177-3

Shapley, R. (1990). Visual sensitivity and parallel retinocortical channels. *Annual Review of Psychology*, 41, 635–658. https://doi.org/10.1146/annurev.psych.41.1.635

Shawkat, F. S., & Kriss, A. (2000). A study of the effects of contrast change on pattern VEPs, and the transition between onset, reversal and offset modes of stimulation. *Documenta Ophthalmologica*, 101(1), 73–89. https://doi.org/10.1023/A:1002750719094

Shevell, S. K., & Kingdom, F. A. A. (2008). Color in Complex Scenes. Annual Review of Psychology, 59(1), 143–166. https://doi.org/10.1146/annurev.psych.59.103006.093619

Souza, G. S., Gomes, B. D., Saito, C. A., da Silva Filho, M., & Silveira, L. C. L. (2007). Spatial Luminance Contrast Sensitivity Measured with Transient VEP: Comparison with Psychophysics and Evidence of Multiple Mechanisms. *Investigative Opthalmology & Visual Science*, 48(7), 3396. https://doi.org/10.1167/iovs.07-0018

Tobimatsu, S., Tomoda, H., & Kato, M. (1995). Parvocellular and magnocellular contributions to visual evoked potentials in humans: stimulation with chromatic and achromatic gratings and apparent motion. *Journal of the neurological sciences*, *134*(1-2), 73-82. https://doi.org/10.1016/0022-510X(95)00222-X

Tobimatsu, S., Tomoda, H., & Kato, M. (1996). Human VEPs to isoluminant chromatic and achromatic sinusoidal gratings: Separation of parvocellular components. Brain Topography, 8(3), 241–243. https://doi.org/10.1007/BF01184777

Tong, F. (2013). Imagery and visual working memory: one and the same? Trends in Cognitive Sciences, 17(10), 489–490. https://doi.org/10.1016/j.tics.2013.08.005

Vidyasagar, T. R., Kulikowski, J. J., Lipnicki, D. M., & Dreher, B. (2002). Convergence of parvocellular and magnocellular information channels in the primary visual cortex of the macaque. *The European journal of neuroscience*, *16*(5), 945–956. https://doi.org/10.1046/j.1460-9568.2002.02137.x

Walsh J. W. T. (1958). *Photometry (3rd ed.)*. London, UK: Constable & Co. Ltd.

Wilken, P., & Ma, W. J. (2004). A detection theory account of change detection. *Journal of Vision*, 4(12), 11. https://doi.org/10.1167/4.12.11

Wuerger, S. M., Ruppertsberg, A., Malek, S., Bertamini, M., & Martinovic, J. (2011). The integration of local chromatic motion signals is sensitive to contrast polarity. Visual Neuroscience, 28(03), 239–246. https://doi.org/10.1017/S0952523811000058

Wyszecki G. Stiles W. S. (1982). Color science: Concepts and methods, quantitative data and formulae (2nd ed.). New York: John Wiley & Sons.

Yin, J., Gao, Z., Jin, X., Ding, X., Liang, J., & Shen, M. (2012). The neural mechanisms of percept–memory comparison in visual working memory. Biological Psychology, 90(1), 71–79. https://doi.org/10.1016/j.biopsycho.2012.02.023

Yörük, H., Santacroce, L. A., & Tamber-Rosenau, B. J. (2020). Reevaluating the sensory recruitment model by manipulating crowding in visual working memory representations. *Psychonomic Bulletin & Review.* https://doi.org/10.3758/s13423-020-01757-0

Zanto, T. P., Rubens, M. T., Thangavel, A., & Gazzaley, A. (2011). Causal role of the prefrontal cortex in top-down modulation of visual processing and working memory. *Nature Neuroscience*, 14(5), 656–661. https://doi.org/10.1038/nn.2773